CRITICAL REVIEW

Check for updates

Luminescent probes for hypochlorous acid *in vitro* and *in vivo*

Shaoqing Dong,[a] Lijuan Zhang,[a] Yanjun Lin, ID *[a] Caifeng Ding ID [b] and Chao Lu ID *[a]

HClO/ClO⁻ is the most effective antibacterial active oxygen in neutrophils. However, its excessive existence often leads to the destruction of human physiological mechanisms. In recent years, the developed luminescent probes for the detection of HClO/ClO⁻ are not only conducive to improve the sensitivity and selectivity of HClO/ClO⁻ detection, but also play a crucial role in understanding the biological functions of HClO/ClO⁻. In addition, luminescent probe-based biological imaging for HClO/ClO⁻ at sub-cellular resolution has become a powerful tool for biopathology and medical diagnostic research. This article reviews a variety of luminescent probes for the detection of HClO/ClO⁻ *in vitro* and *in vivo* with different design principles and mechanisms, including fluorescence, phosphorescence, and chemiluminescence. The photophysical/chemical properties and biological applications of these luminescent probes were outlined. Finally, we summarized the merits and demerits of the developed luminescent probes and discussed their challenges and future development trends. It is hoped that this review can provide some inspiration for the development of luminescent probe-based strategies and to promote the further research of biomedical luminescent probes for HClO/ClO⁻.

Introduction

HClO is mainly generated by the reaction of H_2O_2 and chloride ions in mitochondria.[1] HClO has a pK_a of 7.46, which is in equilibrium with ClO^- under physiological conditions (pH =
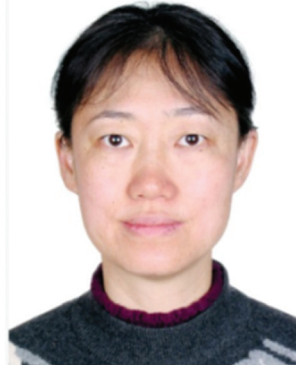
[a]State Key Laboratory of Chemical Resource Engineering, Beijing University of Chemical Technology, Beijing 100029, China. E-mail: linyj@mail.buct.edu.cn, luchao@mail.buct.edu.cn

[b]Key Laboratory of Optic-electric Sensing and Analytical Chemistry for Life Science, Ministry of Education, Qingdao University of Science and Technology, Qingdao 266042, China

7.4).[2] Meanwhile, $HClO/ClO^-$ can cause the host to generate innate immunity when microorganisms invade, and thus $HClO/ClO^-$ is the most effective antimicrobial oxidant for neutrophils.[3] This bactericidal activity is considered to be a key bactericidal effector in natural immunity.[4] Therefore, these inherent features of $HClO/ClO^-$ make it indispensable for cell signaling and immune response.[5] Note that the concentration of $HClO/ClO^-$ from the reaction of H_2O_2 with Cl^- is at the micromolar level.[6] Furthermore, under pathological conditions, the concentration of $HClO/ClO^-$ can even reach millimoles.[7] A high concentration of $HClO/ClO^-$ can simul-

Shaoqing Dong received her BSc degree in Chemistry from Taishan University. In 2015, she began her Ph.D. study at the Beijing University of Chemical Technology under the supervision of Prof. Yanjun Lin and Prof. Chao Lu. Her research involves the synthesis of fluorescent/chemiluminescent nanomaterials, and their analytical applications in chemical and biological systems.

Shaoqing Dong

Lijuan Zhang received her Ph.D. degree in Materials Science from Beijing University of Chemical Technology. She is currently an associate professor at the State Key Laboratory of Chemical Resource Engineering, Beijing University of Chemical Technology. Her areas of interests include nanoscale material sensors and electroanalytical chemistry.

Lijuan Zhang

taneously damage host tissues in the process of destroying invasive microorganisms and cause a series of human diseases, including cardiovascular diseases, inflammatory diseases, acute coronary syndromes, nephropathies, cystic fibrosis and neurodegenerative disorders.[8–10] Meanwhile, due to the short diffusion distance of HClO/ClO⁻ *in vivo* and the presence of multiple antioxidants such as glutathione and amino acids, the detection of endogenous HClO/ClO⁻ is particularly difficult.[11] Therefore, accurate and efficient detection of HClO/ClO⁻ is of great significance to research its physiological and pathological effects on living cells and tissues.

In the past decades, luminescent probes have attracted much attention from researchers.[12–14] The target analytes are identified by a luminescent probe, and the relative substances *in vivo* and *in vitro* are tracked and analyzed by displaying luminescence signals.[15] Recognition of analytes using traditional luminescent probes relies on weak interactions between high-affinity ligands and receptors.[16] However, currently developed luminescent probes mainly detect HClO/ClO⁻ by participating in the formation and fracture of covalent bonds through the corresponding specific recognition sites.[17–19] Recently, metal complexes, semiconductor nanoparticles and up-converting nanophosphates as luminescent nanoprobes are also increasingly being used in the detection of HClO/ClO⁻ using different identification sites on the surface.[20–22] On the other hand, luminescent probe-based bioimaging has become a powerful tool for manipulating living cells and animal microspecies.[23–25] Therefore, luminescent probes can monitor the production of HClO/ClO⁻ with subcellular resolution through bioimaging, and achieve a visualization effect on the biological tissues that produce HClO/ClO⁻.[26,27]

In this review, we summarized the luminescent probes for HClO/ClO⁻ *in vitro* and *in vivo*, including fluorescent, phosphorescent, and chemiluminescent ones. Based on the classification of reactive functional groups (such as sulfur group elements, hydroximic acid, hydrazine, anisidine, *p*-methoxyphenol and unsaturated double bonds), we described the design strategy and photophysical and chemical properties in detail, and introduced the biological applications of luminescent probes. Finally, we summarized the characteristics and limitations of these luminescent probes, and the challenges and future trends of probe development are briefly discussed. It is hoped that this review will provide some inspiration to researchers who develop luminescent probes for HClO/ClO⁻ in clinical medicine and life sciences.

Fluorescent probes for HClO/ClO⁻ detection

Due to simple, fast, and real-time monitoring capabilities, fluorescent probes are often widely used as a general means in the fields of biochemistry, medicine, environmental science, and industries. With the help of high-resolution microscopy technology, important biological substances in cells and tissues can be easily observed.[28,29] In recent years, a lot of fluorescent probes for HClO/ClO⁻ have been reported.[30,31] Based on the oxidation and chlorination of the probe structure and the change of fluorescence intensity, we classified the fluorescent probes for HClO/ClO⁻. Table 1 summarizes the fluorescent probes for HClO/ClO⁻ by comparing their emission wavelengths, detection limits and applications.

Sulfur group elements for HClO/ClO⁻ fluorescence detection

Groups that are electron-donating (–S–, –Se–, –Te– with one electron oxidation potential) are easily oxidized or chloridized to form sulfonates, sulfoxides, selenium oxides, and tellurium oxides. The nucleophilicity of sulfur can be controlled to open the xanthine helix to detect HClO/ClO⁻. In 2007, the first xanthene-based fluorescent probe of the thioether ring compound, HySOx, was found to be highly specific to HClO.[32] In this system, HySOx did not emit fluorescence, but it can react quickly with HClO to form a ring-opening sulfonate derivative HySO₃H (1). During the reaction, the nucleophilicity of the thiol group was reduced, and the helical ring was opened accompanied by strong fluorescence emission. This fluorescent probe was applied to the real-time detection of HClO

Yanjun Lin received his Ph.D. degree in Applied Chemistry from Beijing University of Chemical Technology in 2005. He is currently a full professor at the State Key Laboratory of Chemical Resource Engineering, Beijing University of Chemical Technology. His research interests include nanomaterials and layered and intercalated functional materials.

Yanjun Lin

Caifeng Ding received her Ph.D. degree from Nanjing University of Technology in 2006. She is currently a full professor at the Key Laboratory of Photoelectric Sensing and Life Analysis of Ministry of Education, Qingdao University of Science and Technology. Her research interests include biochemical analysis, photoelectric sensing and nano-biological composite materials.

Caifeng Ding

inside phagosomes. In addition, other thioether ring-based near-infrared fluorescent probes MMSiR (2) and wsMMSiR (3) were designed and synthesized (Scheme 1). These probes had the same reaction progress with HySOx and were used for the *in vivo* imaging of HClO generation in a mouse peritonitis model with low phototoxicity, low autofluorescence, and good tissue penetration, and they were expected to be a useful tool for investigating the wide range of biological functions of HClO.[33]

In 2011, Yoon *et al.* prepared three other rhodamine-based fluorescent probes, R19-S (4), R19-Se (5), and R101-S (6), to increase the number of spiral ring type probes for the imaging of microbe-induced HClO production.[34] With the addition of HClO, the xanthine helix rings of R19-S were opened to form R19-S-Cl and subsequently hydrolyzed to produce carboxylic acid derivatives R19 accompanied by strong fluorescence. The reaction mechanism of the other two probes was the same as that of R19-S. In contrast, R19-Se showed a lower selectivity for HClO, due to the higher susceptibility of selenolactone towards oxidants in comparison with thiolactone of R19-S.[25] The detection limits of the three probes for HClO were evaluated to be 0.4 μM for R19-S, 0.6 μM for R101-S and 2 μM for R19-Se (S/N = 3). Therefore, R19-S exhibited the highest selectivity and sensitivity towards HClO. Polymorphonuclear neutrophils containing R19-S were stimulated using PMA to produce strong fluorescence emission. Therefore, R19-S was used to observe the production of HClO in human PMNs. In addition, R19-S can be used to image HClO production using intestinal epithelial cells of *Drosophila melanogaster* (Fig. 1).

Under the concept of changing sulfur nucleophilicity to obtain a more sensitive HClO probe, Ma *et al.* developed a mitochondrial-targeted RSTPP (7) fluorescent probe for HClO.[35] The thiolactone ring of the RSTPP probe can undergo oxidative cleavage under the action of HClO to generate fluorescence through a desulfurization reaction, enabling the real-time imaging of mitochondrial HClO. In addition, using a rhodamine thiolactone skeleton as the detection group, an STBR (8) ratio fluorescent probe for ClO⁻ was designed on the basis of intramolecular proton transfer in a single excited state.[36] This probe has been used in the live-cell imaging of *Saccharomyces cerevisiae* cells.

Selenium (Se) is an important substance and is often found in the active sites of many enzymes.[37] It also acts as an "anti-oxidant nutrient" that reacts with reactive oxygen species *in vivo*.[38] Accordingly, Se can be used as the reaction site of HClO. Han *et al.* developed a Se-reversible MPhSe-BOD fluorescent probe.[39] Borondipyrromethene (BODIPY) is a fluorescent dye with a high molar absorption coefficient and high fluorescence quantum yield. The connection of borondipyrromethene with 4-methoxylphenylselanyl benzene (MPhSe) could form MPhSe-BOD (9) with weak fluorescence emission as a result of the photoinduced electron transfer process. However, the addition of HClO could break the photoinduced electron transfer process due to the oxidation of Se, and then borondipyrromethene emission was restored. This probe exhibited good permeability to live cells and could monitor intracellular HClO/H₂S redox cycles continuously in RAW264.7 cells. Similarly, Wu *et al.* also designed and synthesized a borondipyrromethene-based HCSe fluorescent probe.[40] Differently, the probe used Se-diphenyl as a modulator to generate a PET effect for the weak fluorescence emission of borondipyrromethene. In view of this principle, PMA-induced endogenous HClO production in RAW264.7 cells was detected. It is worth noting that HCSeO can be reduced to HCSe (10) by glutathione.

The introduction of Se in the conjugated system could lead to a long response time. In order to solve this limitation, Peng *et al.* designed and synthesized a non-conjugated selenium structure cyanine dye-type near-infrared probe SeCy7 (11) by introducing thiamorpholine and selenomorpholine into the structure of heptamethine.[41] Based on the aggregation behavior of heptamethine cyanine dye, the probe exhibited near-infrared absorption and emission characteristics, and it can be used for HClO imaging in living mice with less damage to organisms. The detection principle of this Se containing probe for HClO is shown in Scheme 2.

The elimination of chalcogens can increase the fluorescence intensity of the probe and change the fluorescence emission wavelength and facilitate the design of fluorescent probes for the detection of HClO/ClO⁻ in living organisms (Scheme 3). To this end, Yoon and his coworkers developed a series of ClO⁻ probes.[42–44] For example, they demonstrated that a water-soluble imidazolium salt probe based on imidazoline-2-thione can eliminate sulfur during the reaction and realize the selective detection of HClO/ClO⁻.[42] Furthermore, Yoon's group synthesized imidazoline-2-thione probes, PIS (12) and NIS (13) to yield the corresponding fluorescent imidazolium ions through specific reactions with ClO⁻.[43] PIS can use single photon microscopy image exogenous and endogenous ClO⁻ in HeLa cells and RAW264.7 macrophages. This kind of probe has strong tissue penetrating ability and high spatial

Chao Lu received his Ph.D. degree in Materials Science from the Chinese Academy of Sciences in 2004. He is currently a full professor at the State Key Laboratory of Chemical Resource Engineering, Beijing University of Chemical Technology. In 2011, he was selected to participate in the 'New Century Outstanding Talent' scheme of the Ministry of Education. His research interests are focused on the synthesis and characterization of nanostructured materials, nanosensors, and chemiluminescence. He is responsible for national and international research projects and has published more than 100 papers.
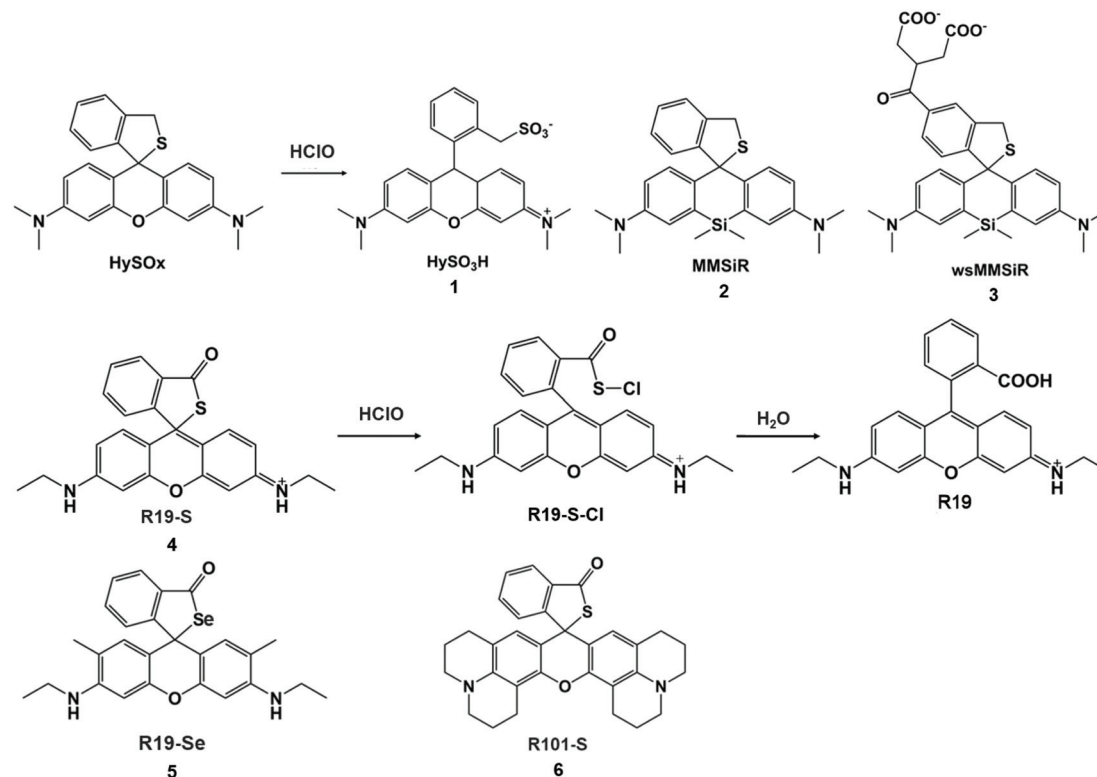
Chao Lu

Table 1 Summary of different fluorescent probes for HClO/ClO⁻ detection

Probes	λ_{em} (nm)	Linear range (μM)	LOD (μM)	Imaging applications	Ref.
HySO₃H (1)	575	—	—	Porcine neutrophil	32
MMSiR (2)	670	0–5	—	Neutrophil and mouse peritonitis	33
wsMMSiR (3)	—	—	—	Neutrophil and mouse	33
R19-S (4)	550	0–12	0.4	Human polymorphonuclear neutrophils and *Drosophila melanogaster*	34
R19-Se (5)	550	0–20	0.6	—	34
R101-S (6)	585	0–10	2	—	34
RSTPP (7)	580	0–35	9×10^{-3}	Raw264.7 cells	35
STBR (8)	I_{590}/I_{514}	0.2–2	0.22	*Saccharomyces cerevisiae* cells	36
MPhSe-BOD (9)	510	0–40	—	Raw264.7 cells	39
HCSe (10)	526	0–9	7.98×10^{-3}	Raw264.7 cells	40
SeCy7 (11)	786	5–60	0.31	Nude mouse	41
PIS (12)	505	—	71×10^{-3}	Raw264.7 cells and a rat hippocampal slice	43
NIS (13)	450	—	—	—	43
PNIS (14)	447	—	0.21	HeLa, astrocytes, HepG2 and Raw264.7 cells	44
MITO-TP (15)	500	—	17.2×10^{-3}	HeLa and Raw264.7 cells	45
LYSO-TP (16)	500	—	19.6×10^{-3}	HeLa and Raw264.7 cells	45
CM1 (17)	480	0–6.4	10×10^{-3}	NIH 3T3, HL-60 and RAW264.7 cells	46
CM2 (18)	468	—	—	—	46
TPFP (19)	538	0–5	5.7×10^{-3}	HeLa cells	47
PM (20)	I_{444}/I_{551}	0–1	1.75	Zebrafish	48
RBH1-UCNPs	554	0–120	0.32	NIH 3T3 cells	49
D1 (21)	575	0–2	40.1×10^{-3}	HeLa cells and zebrafish	51
MitoClO (22)	529	0–40	0.52	MCF-7 cells	52
Probe 1 (23)	556	0–25	0.163	C6 glial and BV2 microglial cells	53
Lyso-HA (24)	I_{585}/I_{450}	0–5	0.11	HeLa and A549 cells	54
FH-HA (25)	580	0–0.01	0.116×10^{-3}	HUVEC, Raw264.7, HeLa, A549, HepG2 cells and zebrafish	59
Rh-ClO (26)	578	40–220	3×10^{-2}	HeLa cells	60
Probe 2 (27)	542	0.5–100	—	HeLa and Raw264.7 cells	61
MitoAR (28)	574	—	—	HeLa and HL-60 cells	62
SNAPF (29)	700	—	—	Human neutrophils, macrophages, human atherosclerotic plaque	63
HA (30)	460, 570	0–32	0.7	HeLa cells	64
BClO (31)	505	0–0.01	0.56×10^{-3}	HeLa, Raw264.7 and MCF-7 cells	68
BRClO (32)	I_{505}/I_{585}, 505	0–100	1.95, 0.59	MCF-7 cells	69
NPs 1 (33)	672	2–20	—	Heart tissue of C57BL/6 mice	76
NPs 2 (34)	470	2–140	—	Raw264.7 cells	77
NPs 3 (35)	430	2–6	0.5	HeLa cells	78
MTPE-M (36)	I_{498}/I_{595}	0–10	0.47	Raw264.7 cells and zebrafish	80
TPE-py-I (37)	I_{592}/I_{720}	1–50	0.25	—	81
ErCSSNPs@Cy925	I_{925}/I_{1525}	0–22	—	Mice	82
NP-2	I_{575}/I_{750}	0–50	—	HeLa cells	83
CD@[Ru(bpy)₃]²⁺	488	0.05–7	0.012	HeLa cells	85
QD-conjugated microbeads	605–595	—	—	Human neutrophil, hepatic leukocyte of rats	87
HKOCl-1 (38)	541	3–8	—	Raw264.7 cells	88
HKOCl-2b (39)	523	—	18×10^{-3}	Raw264.7 cells and THP-1 human macrophages	89
HPs	581–706	0–15	0.4	—	90
Eu(NTA)₃L@PS	I_{618}/I_{496}	0–14	57.3×10^{-3}	—	91
CY-FPA (40)	774	0–9	0.7	A549 cells	92
XWJ (41)	I_{550}/I_{670}	0–55	0.19	Raw264.7 cells	94
BODIPY-Pyra (42)	510	0–50	0.172	MCF-7 and HepG 2 cells	97
NClO (43)	I_{520}/I_{615}	0–30	19×10^{-3}	HeLa cells and zebrafish	98
Py-Cy (44)	I_{470}/I_{613}	—	0.35	HeLa and Raw264.7 cells	99
CMCY (45)	I_{480}/I_{631}	0–73	0.08	HeLa cells	100
SSRN	I_{451}/I_{581}	0–5	52×10^{-3}	HeLa and Raw264.7 cells	101

resolution. The two-photon microscope can also be used to perform ClO⁻ in original 264.7 macrophages and rat hippocampal slices. Similarly, Yoon *et al.* connected a triphenylphosphine mitochondrial target group *via* an ethoxyl chain to modify NIS and formed a new probe, PNIS.[44] The synthesized PNIS (14) probe can image exogenous HClO in HeLa cells,

astrocytes and HepG2 cells, as well as endogenous HClO in macrophages.

To solve the problem of organelle targeting, Chang *et al.* designed a two-photon MITO-TP (15) fluorescent probe for mitochondria and LYSO-TP (16) fluorescent probe for lysosomes.[45] In this system, HClO can effectively remove the

Scheme 1 Structures and mechanisms of thioether ring-based probes for HClO/ClO⁻. Reprinted with permission from ref. 32. Copyright 2007, American Chemical Society. Reprinted with permission from ref. 33. Copyright 2011, American Chemical Society. Reprinted with permission from ref. 34. Copyright 2011, Royal Society of Chemistry.
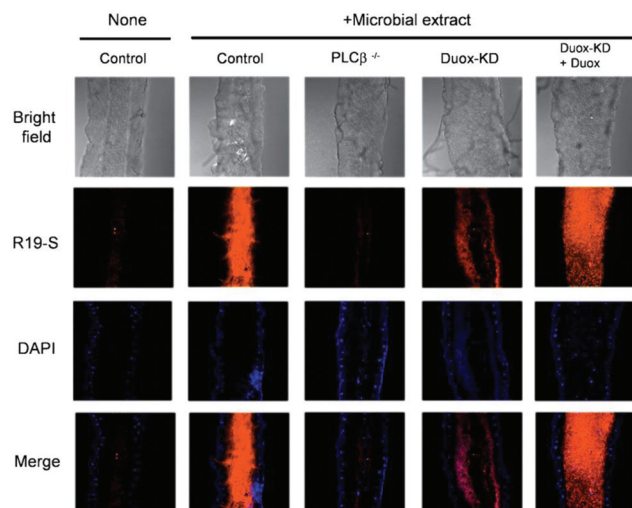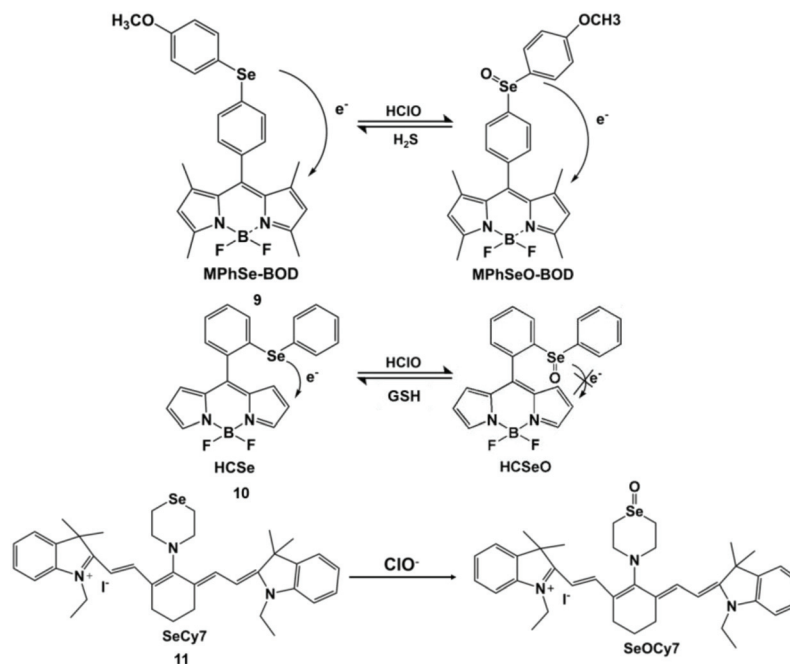

Fig. 1 Detection of DUOX-dependent HClO in the intestinal epithelia of *Drosophila melanogaster* by R19S. Nuclear staining of midgut cells was performed with DAPI (blue). Confocal microscopy images of R19S treated dissected guts from different genotypes with or without oral ingestion of bacterial extract. Reprinted with permission from ref. 34. Copyright 2011, Royal Society of Chemistry.

oxathiolane of thiophene ring-protected naphthylamine to generate the corresponding aldehyde, accompanied by increased fluorescence emissions at 460 nm. These probes

have been used to detect HClO in mitochondria and lysosomes with high sensitivity.

Jiang *et al.* synthesized CM1 (17) and CM2 (18) fluorescent probes by the reduction of coumarin dyes and subsequent selenylation, and observed the generation of endogenous HClO/ClO⁻ in progenitor cells and macrophages.[46] During the reaction, selenium was first oxygenated, and then coumarin fluorophores are formed by the elimination reaction. This probe has the merits of high selectivity, high sensitivity, and fast response speed, is independent of pH and was applied to the detection of HClO/ClO⁻ in aqueous media and living cells.

Chen *et al.* also designed two-photon fluorescent probe TPFP (19) through the integration of the lysosome-targetable group (aminoethyl)morpholine, two-photon fluorophore 1,8-naphthalimide and HClO capturing phenyl-thiourea together for lysosome-targetable HClO detection.[47] The PET process of TPFP was inhibited by HClO-mediated S atomic oxidation and the green fluorescence of 1,8-naphthalimide recovery. The LOD of this probe was lower than that of LYSO-TP. Based on the same naphthalimide group, they further researched the probe that was used to detect HClO *in vivo*. In addition, a polymer micelle-based ratiometric fluorescent probe PM (20) was synthesized using amphiphilic diblock copolymers [PEO$_{113}$-*b*-P(St$_{20}$-*co*-NPAI$_3$)] *via* reversible addition-fragmentation chain transfer radical polymerization.[48] Upon the addition of HClO, thiourea transformed into an imidazoline derivative, which

Scheme 2 Structures and mechanisms of Se-containing probes for HClO/ClO⁻. Reprinted with permission from ref. 39. Copyright 2013, Royal Society of Chemistry. Reprinted with permission from ref. 40. Copyright 2013, American Chemical Society. Reprinted with permission from ref. 41. Copyright 2014, Royal Society of Chemistry.

Scheme 3 Structures of chalcogen-containing probes and reaction mechanisms for HClO/ClO⁻ based on chalcogen elimination. Reprinted with permission from ref. 43. Copyright 2015, Wiley. Reprinted with permission from ref. 44. Copyright 2016, American Chemical Society. Reprinted with permission from ref. 45. Copyright 2015, American Chemical Society. Reprinted with permission from ref. 46. Copyright 2013, American Chemical Society. Reprinted with permission from ref. 47. Copyright 2018, Elsevier. Reprinted with permission from ref. 48. Copyright 2018, Elsevier.

Fig. 2 Synthesis of rhodamine-modified up-conversion nanophosphors and the proposed recognition mechanism towards HClO. Reprinted with permission from ref. 49. Copyright 2014, Wiley.

suppressed intramolecular charge transfer and promoted FRET, causing the changes of fluorescence emission ratiometric. This phenomenon of probe selectively visualized endogenous HClO in zebrafish during lipopolysaccharide-induced acute liver injury.

In 2014, Zhang *et al.* developed rhodamine-modified up-conversion nanophosphors (NaYF$_4$: 20 mol% Yb, 1.8 mol% Er, 0.5 mol% Tm) for HClO sensing (Fig. 2).[49] The polyacrylic acid-modified up-conversion nanophosphors were used as the carrier of the RBH1 probe to detect HClO through the luminescence resonance energy transfer process between up-conversion nanophosphors and RBH1. The sulfur elements on thiosemicarbazide were eliminated after they interacted with HClO. As a result, the green up-conversion luminous intensity at 554 nm increased gradually, and the emission in the near-infrared region was almost unchanged. Therefore, this probe could be used for the ratiometric up-conversion luminescence visualization of HClO released by MPO-mediated peroxidation of chloride ions in living cells.

Nitrogen-containing functional groups for HClO/ClO⁻ fluorescence detection

Nitrogen-containing functional groups, such as hydroximic acid, hydrazine/hydrazone and anisidine, can react specifically with HClO/ClO⁻. HClO-promoted oxidation of hydroxamic acid can prohibit the decay process of the excited state of C=N bond isomerization, resulting in the strong fluorescent production of the probe derivative.[50] According to a similar principle, a series of hydroxamic acid-based fluorescent probes were prepared for the detection of HClO (Scheme 4).[51–53] Li and his coworkers developed a hydroxyl oxime-based fluorescent probe D1 (21) through the hydroxylamine hydrochloride treatment of 6-dimethylamino-3-hydroxynaphthalene-2-carbaldehyde to image ClO⁻ in the lysosome of organisms.[51] The oxime moiety of D1 can react rapidly (<10 s) with ClO⁻ to

Scheme 4 Structures and mechanisms of hydroxamic acid-based probes for HClO/ClO⁻. Reprinted with permission from ref. 51. Copyright 2019, Wiley. Reprinted with permission from ref. 52. Copyright 2013, Royal Society of Chemistry. Reprinted with permission from ref. 53. Copyright 2014, Royal Society of Chemistry.
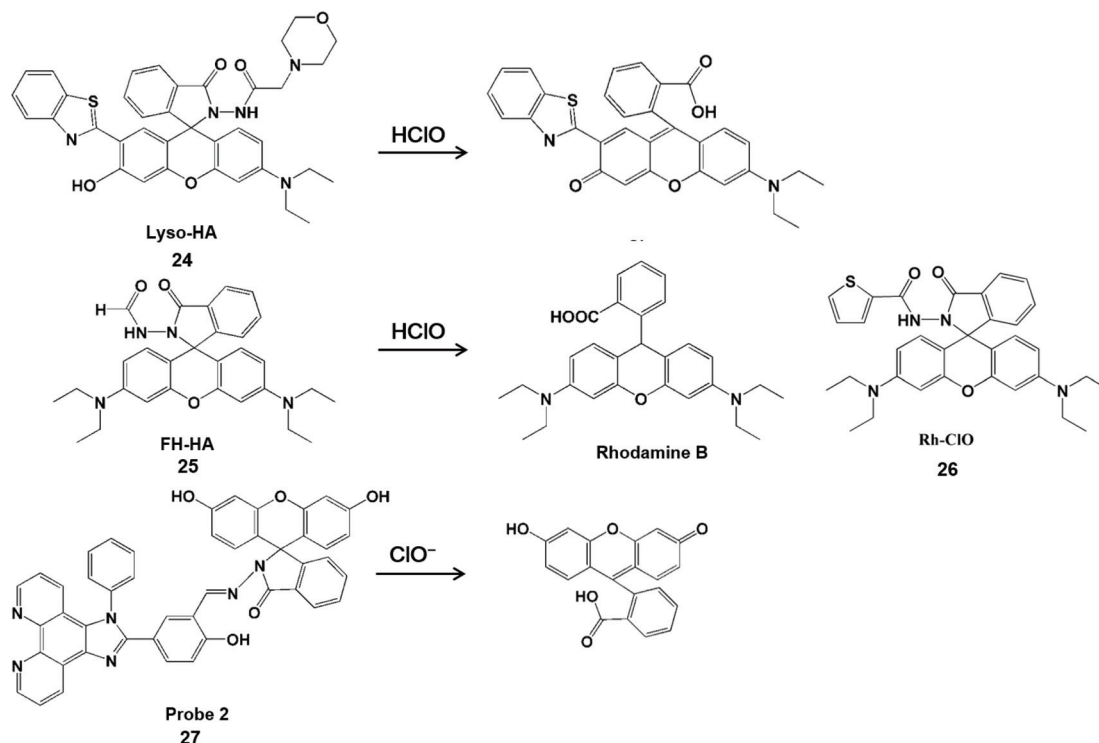
provide the corresponding strong fluorescent aldehyde product 2, and thus product 2 was used for monitoring changes in ClO⁻ levels both in HeLa cells and in zebrafish with the aid of fluorescence microscopy. It was worth noting that aldehyde product 2 with excellent optical stability can be used to detect ClO⁻ in real samples at −78 °C. Analogously, BODIPY-based probe MitoClO (22) was obtained by introducing the oxime group at the 2-position of BODIPY.[52] Through the HClO-induced nonradiative deactivation of C=N isomeri-

zation, the generated MitoCOOH fluorescence was observed to be enhanced by 35-fold. In addition, triphenylphosphine (a classic subcellular locating group) was introduced at the *meso*-position to enable this probe to detect HClO inside mitochondria. In 2014, Kumar *et al.* designed a dimethyl-aminocinnamaldehyde linked oxime-based fluorescent probe 1 (23).[53] It was demonstrated that the oxime group can undergo the oxidation of HClO to convert nitrile oxide, generating a fluorescent emission band at 556 nm. With this interesting reaction, this probe was used to image endogenous ClO$^-$ produced by LPS-stimulated C6 glioma cells and BV2 microglial cells.

Hydrazine/phenylhydrazine-modified spirolactam is also HClO-activatable (Scheme 5). Lin *et al.* developed a lysosomal-targeted ratiometric fluorescent HClO probe Lyso-HA (24).[54] In comparison with fluorescence resonance energy transfer-based probes,[55] this design strategy did not require a connector and provider. The fluorescence detection of HClO was performed by blocking the process of excited-state intramolecular proton transfer with proton-free benzothiazole. Moreover, this probe had a good ratio signal (I_{586}/I_{450}) resolution and membrane permeability. These merits facilitated it to enable the imaging of endogenous and exogenous HClO in living cells. Unfortunately, this type of probe can also be used to identify ONOO$^-$.[56–58] To improve the specificity towards HClO detection, Sheng *et al.* attached an electron-withdrawing formyl

group at the amino position of the probe to construct a rhodamine-formylhydrazine type fluorescent probe FH-HA (25).[59] Similarly, Rh-ClO (26) probes have rhodamine-formylhydrazine structures in accordance with FH-HA, which can detect HClO in mitochondria.[60] The fluorescence of rhodamine B was released by HClO-mediated ring-opening of the probe. Therefore, this probe can provide direct visualization of HClO in living cells and zebrafish with low cytotoxicity and high sensitivity. In addition, this probe can also distinguish cancer cells from normal cells by monitoring basal HClO in cancer cells. In 2017, Lv *et al.* synthesized a new probe 2 (27) for HClO with the spirolactam form of fluorescein.[61] The HClO-promoted ring-opening of the probe could lead to fluorescence emission enhancement at 542 nm. With the aid of flow cytometry, this probe realized the quantitative detection of intracellular HClO by recording the intensity changes of fluorescence emissions.

HClO-mediated the cleavage of *p*-anisidine (4-aminophenylether) and can enhance fluorescence by releasing aniline oxygroups that block the photoinduced electron transfer process. Therefore, it can be used as a fluorescent probes for the detection of HClO (Scheme 6).[62–64] Nagano *et al.* synthesized a MitoAR (28) and MitoHR fluorescent probe by introducing the 4-amino and 4-hydroxylphenylether electron donor into the 2-position phenyl moiety of rhodamine, respectively.[62] The positive charge of rhodamine dye can promote the movement

Scheme 5 Structure of probes containing hydrazine or phenylhydrazine modified spironolactone and mechanism of detection of HClO/ClO$^-$. Reprinted with permission from ref. 54. Copyright 2016, Royal Society of Chemistry. Reprinted with permission from ref. 59. Copyright 2019, American Chemical Society. Reprinted with permission from ref. 60. Copyright 2018, Elsevier. Reprinted with permission from ref. 61. Copyright 2017, American Chemical Society.
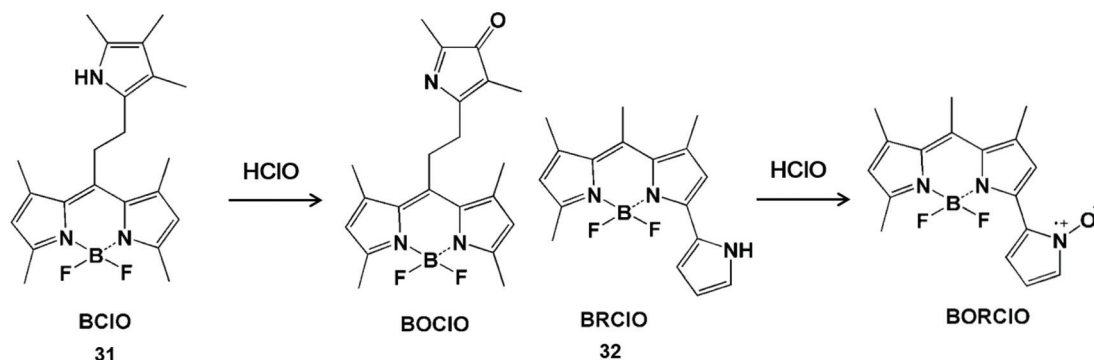
Scheme 6 Structures and mechanism of *p*-anisidine-based probes for HClO/ClO⁻. Reprinted with permission from ref. 62. Copyright 2007, American Chemical Society. Reprinted with permission from ref. 63. Copyright 2007, Elsevier. Reprinted with permission from ref. 64. Copyright 2013, Royal Society of Chemistry.
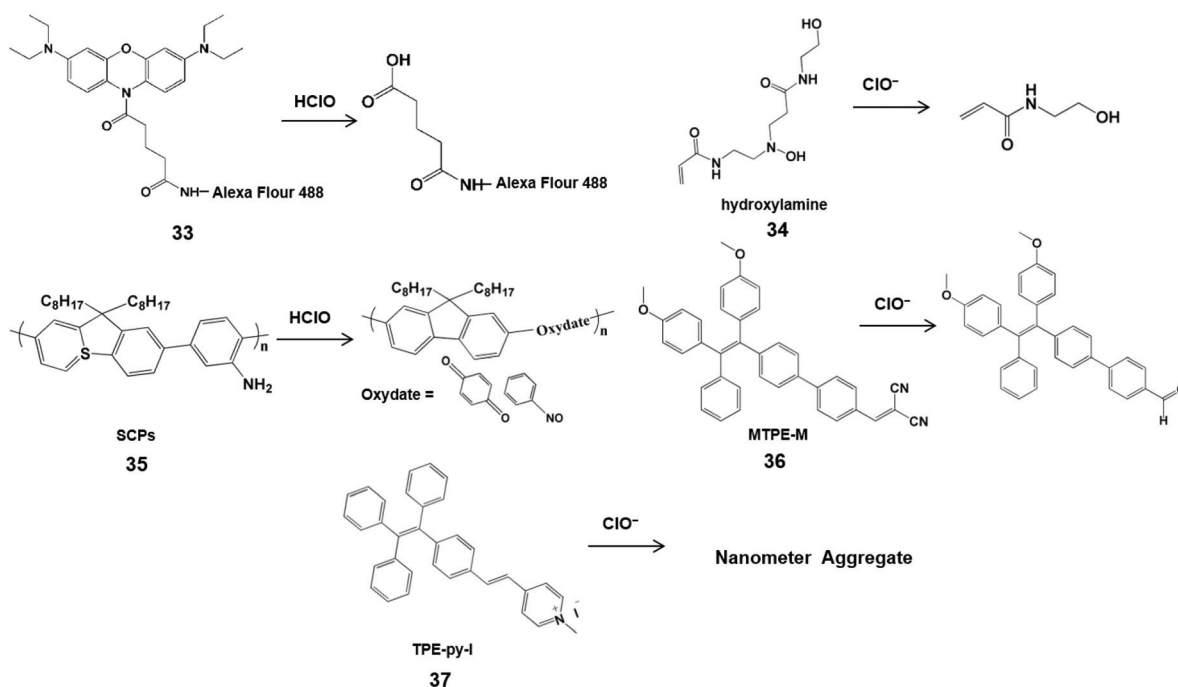
of phospholipid bilayers into the cell and accumulation into the mitochondrial matrix through the negative membrane potential. The fixed position of the electron donor was close to xanthine, which was conducive to the HClO-mediated PET process to regulate the fluorescence of the rhodamine-containing probe. The high fluorescence HMTMR used to indicate HClO was obtained by the cleavage of the oxidized ether moiety in MitoAR or MitoHR. This probe was distributed in mitochondria after internalization and thus it can realize the visualization of HClO inside mitochondria in HeLa cells. In addition, Libby *et al.* have developed a powerful near-infrared sulfonaphthoaminophenyl fluorescein fluorescent probe SNAPF (29) with a xanthene-based dye scaffold on the basis of the same principle.[63] After the probe was oxidized, sulfonaphthoaminophenyl dye with 676 nm emission was produced, which was used as an indicator for HClO detection. For the sake of the good selectivity and sensitivity, this probe can image HClO produced by stimulated MPO-expressing cells, as well as HClO from bone marrow-derived macrophages. Furthermore, with the aid of fluorescence reflection imaging, this probe can directly observe the HClO-mediated inflammatory tissue damage in mice and HClO production by MPO expressing cells in human atherosclerotic arterial samples in a noninvasive manner. In comparison with the traditional methods, sulfonaphthoaminophenyl fluorescein-assisted molecular imaging technology can further aid in understanding the function and dynamic process of HClO in vascular diseases, which is conducive to accelerating the clinical diagnosis process. In general, multi-emission fluorescent probes could self-calibrate the interference factors and improve detection

accuracy. Accordingly, a dual-emitting fluorescent probe HA (30) was synthesized by tethering 4-aminophenoxyl to 1,8-naphthalimide *via* a carbamate linkage.[64] The 4-Aminophenol moiety of HA is electron-rich and it can quench fluorescence *via* the PET mechanism. After interaction with ClO⁻, two acylation derivatives with the HA-1 and HA-3 configuration were formed and the distinct fluorescent emission bands were observed at 460 nm and 570 nm, respectively. Since the fluorescence of the probe has good water-solubility and inertness under physiological conditions, it has been developed for the dual-channel fluorescence imaging of ClO⁻ in living cells.

Pyrrole can act as the single-atom electron donor to reduce the intensity of background fluorescence of the probe and improve the signal-to-noise ratio by enhancing the photo-induced electron transfer effect (Scheme 7).[65–67] The interruption of the photoinduced electron transfer process in the fluorescent probes has been used for HClO detection.[68,69] In 2014, Peng *et al.* synthesized a BODIPY-based HClO probe BClO (31) by the Michael addition reaction of acryloyl chloride with a 2,4-dimethylpyrrole fragment.[68] The pyrrole group at the *meso* position had an enhanced photoinduced electron transfer effect on the BODIPY fluorophore, so as to obtain low background fluorescence and a high signal-to-noise ratio. This probe can be applied to image basal HClO in cancer cells and monitor the time-dependent elevation of HClO generated by MCF-7 cells. Furthermore, they also synthesized a BODIPY-based ratiometric fluorescent probe BRClO (32) for improving the detection accuracy of HClO.[69] The corresponding oxynitride product was formed by HClO oxidation, resulting in a blue shift of the emission wavelength. Due to the excellent
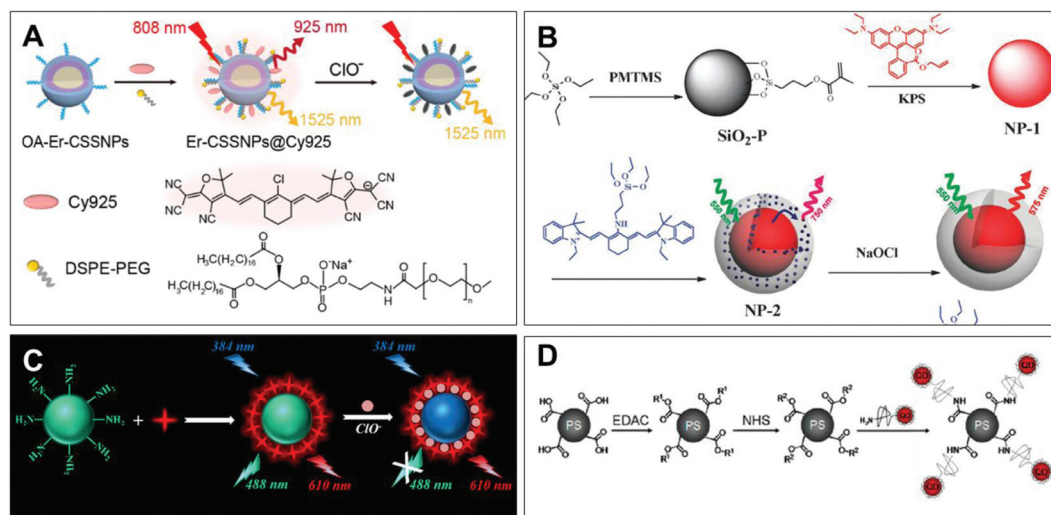
Scheme 7 Structures and mechanism of pyrrole-containing probes for HClO/ClO⁻. Reprinted with permission from ref. 68. Copyright 2014, American Chemical Society. Reprinted with permission from ref. 69. Copyright 2015, American Chemical Society.

Scheme 8 Structures and mechanism of nitrogen-containing functional groups in HClO/ClO⁻ nanoprobes. Reprinted with permission from ref. 76. Copyright 2009, American Chemical Society. Reprinted with permission from ref. 77. Copyright 2013, Wiley. Reprinted with permission from ref. 78. Copyright 2015, Royal Society of Chemistry. Reprinted with permission from ref. 80. Copyright 2016, Royal Society of Chemistry. Reprinted with permission from ref. 81. Copyright 2020, Elsevier.

sensing properties and biocompatibility, the ratio fluorescent emission of this probe was applied to detect HClO changes in the presence of exogenous HClO in live cells with clearly separated signals.

With the characteristics of easy modification and good biocompatibility, nanoprobes can be designed as nanoparticles with a large number of high-sensitivity luminescent groups to replace small-molecule probes, and have been widely used in the field of biology.[70,71] In addition, nanoprobes were conducive to store in the targeted lesion tissue, enabling them to identify reactive oxygen species.[72] To date, a variety of nano-

probes have been prepared for HClO measurement *in vivo*.[73] Most of them utilized nitrogen-containing groups as the specific identification sites for sensing HClO/ClO⁻ (Scheme 8 and Fig. 3).

Magnetic nanoparticles have been applied to the human body due to their good biocompatibility and since they facilitate bioimaging.[74,75] Hilderbrand *et al.* developed non-luminescent organic conjugated nanoprobes by attaching fluorogenic oxazine to Alexa Flour 488 modified magnetic nanoparticles 1 (33) for HClO visualization *in vivo*.[76] HClO can activate the nanoprobe and release oxazine dye from the nano-

Fig. 3 Structures and mechanism of the nitrogen-containing nanoprobe in HClO/ClO⁻. (A) Reprinted with permission from ref. 82. Copyright 2019, American Chemical Society. (B) Reprinted with permission from ref. 83. Copyright 2012, Royal Society of Chemistry. (C) Reprinted with permission from ref. 85. Copyright 2017, American Chemical Society. (D) Reprinted with permission from ref. 87. Copyright 2011, American Chemical Society.
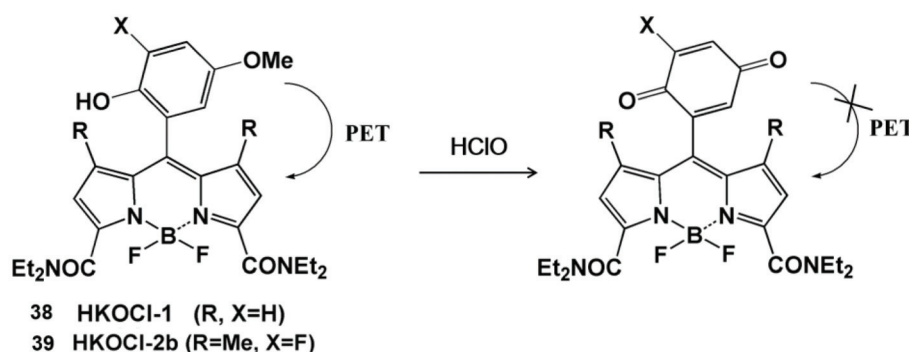
particle scaffold to restore its fluorescence properties. In addition, the attachment of hundreds of oxazine could alter the elution kinetics of small oxazines and prolong the half-life of the circulating probe, resulting in a high sensitivity towards HClO. Therefore, this nanoprobe can image HClO produced by ischemia-induced inflammation and cardiovascular disease in living cells and in mice. In addition, Lin *et al.* utilized poly (-aminoamine) dendrimers to synthesize an organic polymer nanoprobe 2 (34) for ClO⁻ sensing.[77] Through a cascade of oxidations in the tertiary amine of the dendritic cores, poly(-aminoamine) dendrimers generated fluorescent hydroxylamine, which can be selectively destroyed by ClO⁻ to shut down the fluorescence at 470 nm. This kind of simple sensing system can utilize confocal microscopy for ClO⁻ imaging in macrophages with minimal interference from biological matrixes, and is expected to be a sensing tool for ClO⁻ in biological fluids.

Semiconductor π-conjugated polymer (SCP) nanoparticles have strong light emission and low biological toxicity compared with traditional organic molecule and inorganic semiconductor quantum dots. Taking into account these merits, Tang *et al.* synthesized an amine-functionalized SCP nanoprobe 3 (35) composed of polyfluorene derivatives for the determination of HClO.[78] Through the oxidation of HClO, the aniline units of polyfluorene derivatives generated oxydate. Simultaneously, the conjugation in the semiconducting conjugated polymer backbone was destroyed, accompanied by an obvious fluorescence quenching at 419 nm. With the rapid response and photo/chemical stability, this nanoprobe was used to image HClO in HeLa cells.

Many fluorescent molecules have the phenomena of aggregation induced quenching in aqueous media or physiological buffers, severely impairing their luminescence emission and sensing performances.[79] To effectively avoid this phenomenon, Wu *et al.* designed an aggregation induced emission-based

ratiometric fluorescent nanoprobe MTPE-M (36) for intracellular ClO⁻ imaging.[80] In this probe, electron-withdrawing group dicyanovinyl was linked to C=C, resulting in a highly electron-deficient site that is more vulnerable to attacks by the nucleophile ClO⁻. Meanwhile, the aggregation of probe molecules could easily form micelle nanoparticles with red fluorescence emission. Therefore, ClO⁻ could trigger the conversion of dicyanovinyl tetraphenylethene to the aldehyde tetraphenylethene, leading to the blue shift of fluorescence emission. The change of ratio fluorescence signals allowed the probe to image endogenous ClO⁻ in living cells and zebrafish with the advantages of fast response, high sensitivity and good selectivity. Another AIE ratiometric nanoprobe 1-methyl-4-(4-(1,2,2-triphenylvinyl)styryl) pyridin-1-ium iodide TPE-py-I (37) was used for detecting ClO⁻ in tap and pond water.[81] Of note, the positive charge of the probe can be balanced by the electrostatic interaction between ClO⁻ and pyridine salt groups, and the nanometer aggregates are formed, accompanied by the change from reddish to bright yellow.

Li *et al.* synthesized the dual near-infrared ratiometric nanoprobe Er-CSSNPS@Cy925 by combining the Cy925 cyanine dye that can recognize ClO⁻ with NaYbF₄:NaYF₄:Yb:Nd nanoparticles in living organisms (Fig. 3A).[82] By the structure of nitrogen-containing dye Cy925 gradually degrading, the NIR peaks at 925 nm were decreased. The NIR ratio ($I_{925 nm}/I_{1525 nm}$) of the cyanogroup dye and the nanoparticle represented the interaction with ClO⁻. Based on these good near-infrared ratiometric signals, deeper imaging penetrability and lower autofluorescence, the probe can detect the change in concentration of ClO⁻ in mice limbs with arthritis through *in vivo* imaging experiments. In addition, Peng *et al.* established the first FRET ratiometric fluorescent nanoprobe NP-2 for ClO⁻ (Fig. 3B).[83] Through Stöber synthesis and a copolymerization reaction, NP-2 was obtained *via* embedding an amino cyanine dye and rhodamine B in SiO₂. The specific response of ClO⁻ was achieved by the substitution of aliphatic
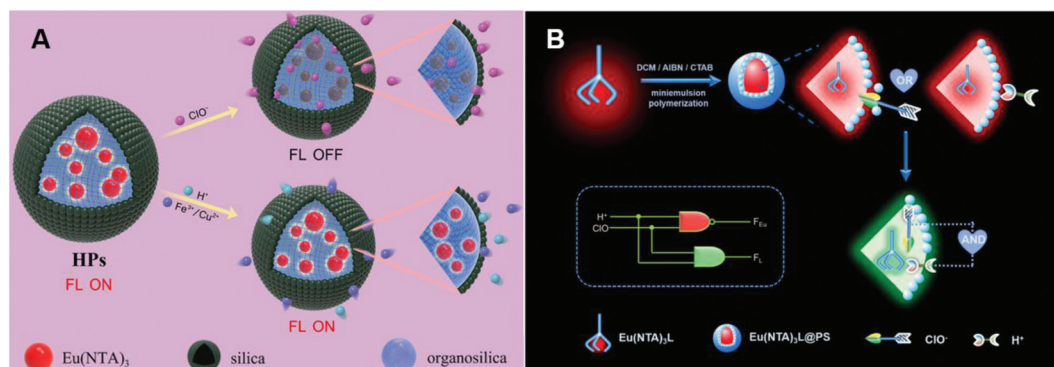
Fig. 4 Structures and mechanism of the oxygen-containing function group nanoprobe in HClO/ClO⁻. (A) Reprinted with permission from ref. 90. Copyright 2019, Elsevier. (B) Reprinted with permission from ref. 91. Copyright 2020, Elsevier.

Wang *et al.* synthesized a near-infrared fluorescent probe CY-FPA (40) by covalently connecting an electron-donating group to the cyano main chain for HClO detection.[92] The quenching of near-infrared fluorescence was derived from the formation and degradation of chlorohydrin as well as the formation of epoxy during the reaction. In addition, this probe has good water solubility, photobleaching resistance and cell-membrane permeability, and can be further used for near-infrared fluorescence imaging of HClO in living cells.
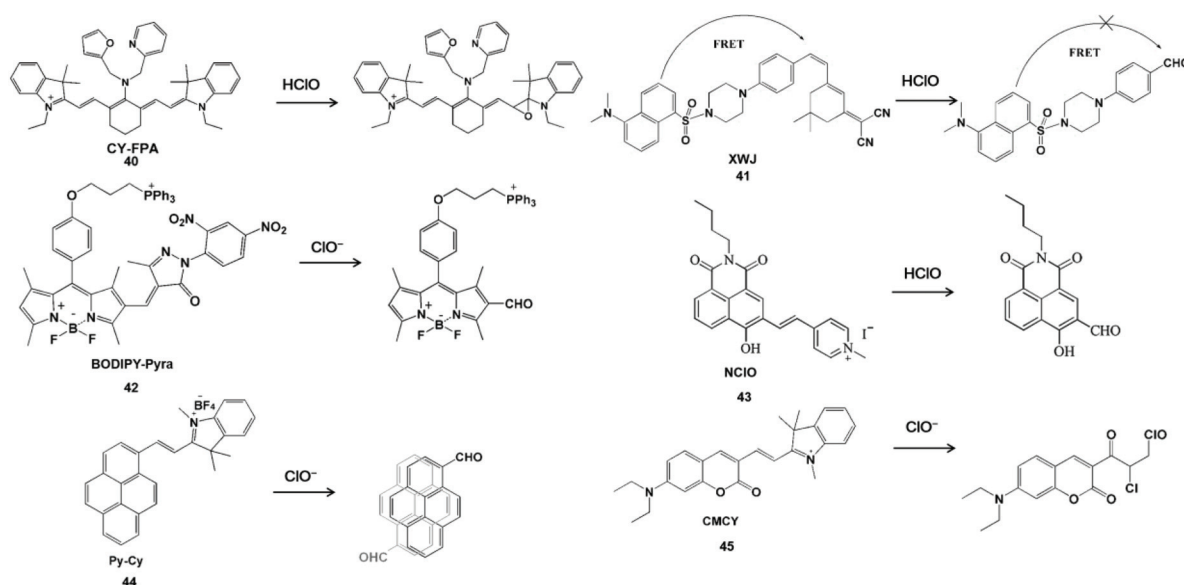
The ratiometric fluorescent probe can avoid the influence of other variables such as instrument efficiency, excitation intensity and environmental effects for reasonable built-in rectification.[93] Zhao *et al.* constructed a FRET-based ratiometric fluorescent probe XWJ (41) using dansyl and 2-(3,5,5-trimethyl-cyclohex-2-en-1-ylidene) malononitrile for sensing HClO.[94] In this system, the dansyl fluorophore can be used to construct the FRET dyad and the near-infrared fluorescence of 2-(3,5,5-trimethylcyclohex-2-en-1-ylidene) malononitrile could provide the fluorescence energy conversion system.[95,96] Upon the addition of HClO, the C=C double bonds were cleaved to yield an aldehyde group and the FRET was turn off, resulting in a well-separated double emission. This ratiometric probe was used to image endogenous and exogenous HClO in living cells with outstanding sensitivity and selectivity. In addition, Qian *et al.* utilized α,β-unsaturated pyrazolone to synthesize a probe BODIPY-Pyra (42) for the real-time monitoring of HClO in organisms.[97] According to the same rationale, the BODIPY-CHO product could generate green emission at 510 nm. This probe was realized for HClO fluorescent imaging in MCF-7 cells, HepG 2 cells and zebrafish. Long wavelength photons can deeply penetrate tissues and a large Stokes shift can avoid the self-absorption issue. Yang *et al.* developed a long wavelength emission probe NClO (43) based on a naphthalimide derivative.[98] The C=C double bond between naphthalimide and methylated pyridine in the probe could be oxidized by HClO with a blue shift of emission to display a ratiometric fluorescence change. NClO can detect HClO in living cells and zebrafish by fluorescence images. Wu *et al.* synthesized a near-infrared ratiometric fluorescent probe Py-Cy

(44) for HClO determination.[99] The red emission probe extended the conjugation length and introduced the D-π-A electronic structure by the Norman Geler reaction. The pyrene derivative fluorophore was converted to pyrene-CHO-based excimer after the reaction with ClO⁻, resulting in blue fluorescent emission. The introduction of BF_4^- could improve the light stability and water solubility, the probe could be used to image ClO⁻ produced in RAW264.7 cells. Hu *et al.* constructed a fluorescent probe CMCY (45) by connecting diethylaminocoumarin aldehyde with 1,2,3,3-tetramethyl-3*H*-indolium iodine for sensing ClO⁻.[100] This probe showed the maximum emission at 631 nm. HClO readily reacted with C=C double bonds and destroyed the large π-conjugate of the probe, resulting in the formation of chlorides with blue fluorescence emission. With good membrane permeability, the probe could be used for the real-time sensing of ClO⁻ in HeLa cells using confocal fluorescence microscopy. The principle of the above-mentioned C=C double bond-containing probe to generate aldehyde derivatives during detecting HClO/ClO⁻ is shown in Scheme 10.

Chen *et al.* prepared a fluorescent nanoprobe SSRN by coprecipitation of the morpholine moiety modified amphiphilic polymers with a single dye for ratiometric monitoring HClO in HeLa and macrophage cells (Fig. 5).[101] In comparison with the FRET-based probe for donor-recipient separation, SSRN integrated both the referenced unit and HClO sensing unit into a single dye to achieve the self-referenced ratiometric effect by intramolecular charge transfer. The Cl atom of HClO can lead to the opening of the C=C double bond through the addition reaction, resulting in the heavy atomic effect of chlorine and thereby reducing the fluorescence emission at 581 nm. In addition, this probe was able to visualize exogenous and endogenous HClO in lysosomes by utilizing the localization ability of morpholine molecules.

Phosphorescent probes for HClO/ ClO⁻ detection

In recent years, phosphorescent probes have attracted considerable attention owing to their excellent optical stability.[102] In comparison with fluorescent probes, phosphorescent

Scheme 10 Structures and mechanism of C=C unsaturated double bonds for HClO/ClO⁻ probes. Reprinted with permission from ref. 92. Copyright 2014, American Chemical Society. Reprinted with permission from ref. 94. Copyright 2014, American Chemical Society. Reprinted with permission from ref. 97. Copyright 2019, Elsevier. Reprinted with permission from ref. 98. Copyright 2019, Elsevier. Reprinted with permission from ref. 99. Copyright 2016, American Chemical Society. Reprinted with permission from ref. 100. Copyright 2014, Royal Society of Chemistry.

Fig. 5 Structures and mechanism for the selective visualization of lysosomal HClO by the SSRN nanoprobe. Reprinted with permission from ref. 101. Copyright 2020, Elsevier.

probes rarely suffer from internal filtering and homo-FRET effects due to the large Stokes shift.[103] In addition, the long-lived luminescence generated by the spin-forbidden nature can be used in time-resolved imaging to minimize self-fluorescence interference and improve imaging accuracy.[104] A number of phosphorescent probes with HClO/ClO⁻ specific recognition groups have been reported.[105] According to the different structures and luminescence characteristics of the probes, Table 2 summarizes the phosphorescent probes for HClO/ClO⁻ by comparing their emission wavelengths, detection limits and corresponding applications.

Sulfur group elements for HClO/ClO⁻ phosphorescence detection

HClO-promoted S elimination in the probe could inhibit the photoinduced electron transfer process, accompanied by phosphorescence enhancement (Scheme 11). Hence, Yuan *et al.* synthesized a Ru(II) complex-based luminescent probe [Ru(bpy)₂(DNPS-bpy)]-(PF₆)₂ (46) by exploiting a "signaling moiety-recognition linker quencher" sandwich approach.[106] On account of the photoinduced electron transfer effect from the Ru(II) center to the 2,4-dinitrophenyl electron acceptor, the luminescence of the probe was completely withheld. Upon the

Table 2 Summary of different phosphorescent probes for HClO/ClO⁻ detection

Probe	λ_{em} (nm)	Linear range (μM)	LOD (μM)	Imaging application	Ref.
[Ru(bpy)$_2$ (DNPS-bpy)]-(PF$_6$)$_2$ (46)	626	2.5–50	53.5×10^{-3}	HeLa and Raw264.7 cell	106
Mito-NPSTTA-Eu^{3+} (47)	610	0.005–0.1	1.8×10^{-3}	Raw264.7 cell, HepG2 cells and zebrafish	107
[Ru (bpy)$_3$$^{2+}$]-PTZ (48)	605	10^{-3}–100	1.8×10^{-5}	Mice	108
Ru-Fc (49)	626	2–15	38.6×10^{-3}	MDA-MB-231 cells, Daphnia Magna	109
Ir-Fc (50)	600	5–40	93.3×10^{-3}	HepG 2 cells and zebrafish	110
Ruazo (51)	600	0.5–50	0.437	Mice	111
Ir1-Ir4 (52)	534–598	—	—	Raw264.7 cell	112
SiO$_2$-1@mSiO$_2$-2 (53)	I_{598}/I_{500}	0–50	—	Raw264.7 cell	113
ANMTTA-Eu^{3+} (54)	610	0.01–1	1.3×10^{-3}	HeLa and Raw264.7 cell	114
ANMTTA-Tb^{3+} (55)	540	0.01–1	0.64×10^{-3}	—	114
[Ru(bpy)$_2$(AN-bpy)]$^{2+}$ (56)	612	2.5–40	33×10^{-3}	HeLa and porcine neutrophils cell	115
RTLNP	I_{539}/I_{607}	—	0.27	Raw264.7 cell, zebrafish and Daphnia Magna	116
Ru-1 (57)	587	0–400	76×10^{-3}	HEK293T cells	117
NPPTTA-Eu^{3+} (58)	610	0.01–0.06	1.1×10^{-3}	Raw264.7 cell and Daphnia Magna	118

Scheme 11 Structures of sulfur-containing probes and reaction mechanisms for HClO/ClO⁻ based on sulfur elimination. Reprinted with permission from ref. 106. Copyright 2013, American Chemical Society. Reprinted with permission from ref. 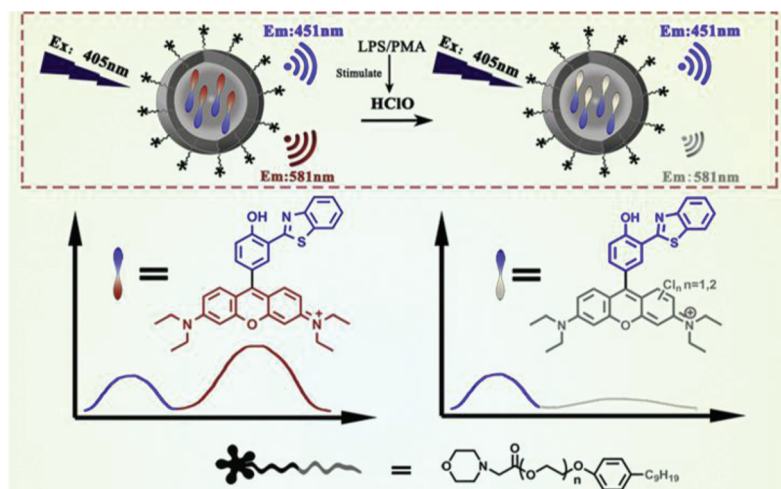107. Copyright 2017, Royal Society of Chemistry. Reprinted with permission from ref. 108. Copyright 2014, Royal Society of Chemistry.

addition of HClO, 2,4-dinitrophenyl was separated from the Ru(ɪɪ) complex with remarkable red emissions. Moreover, the probe can be used to capture and visualize exogenous/ endogenous HClO inside cancer and macrophages cells. Analogously, Yuan *et al.* prepared a mitochondria-targeting time-gated luminescent probe Mito-NPSTTA-Eu^{3+} (47) for sensing HClO.[107] The long-lived red luminescence signals were observed when this probe interacted with HClO. The high sensitivity and selectivity of the probe can be used for the imaging of mitochondrial HClO in RAW264.7 cells and zebrafish.

ClO⁻-responsive phenothiazine is a typical S-containing compound with a reversible one-electron oxidation potential. In view of this feature, Sun *et al.* designed an intramolecular electron transfer phosphorescent probe [Ru(bpy)$_3$$^{2+}$]-phenothiazine (48) through a ruthenium tris-bipyridyl complex covalently linked with phenothiazine.[108] The phosphorescence intensity of the probe oxidized by ClO⁻ was significantly enhanced at 605 nm. However, after H$_2$S was added in sequence, the probe returned to the original state. This probe showed good redox reversibility and enabled one to monitor ClO⁻/H$_2$S simultaneously. In this end, it was used to visualize
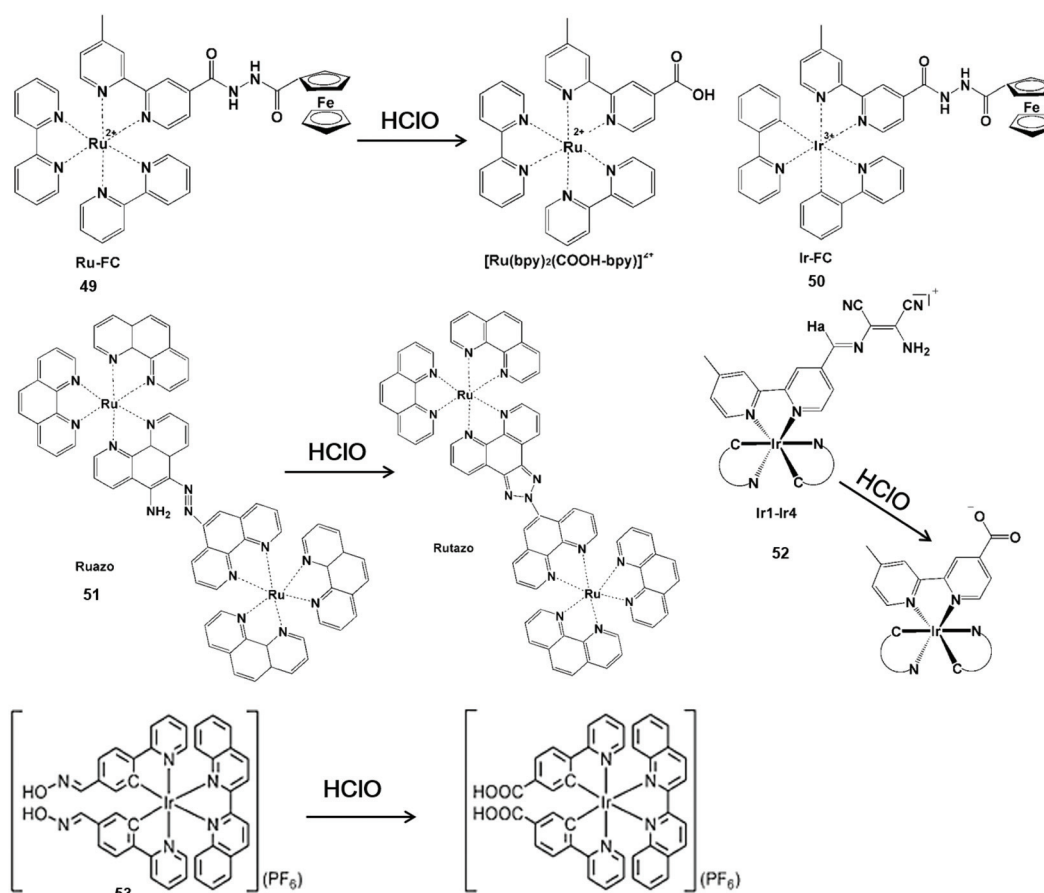
the ClO⁻ and H$_2$S-induced redox cycle in mice at the subcellular level by imaging technology.

Nitrogen-containing functional groups for HClO/ClO⁻ phosphorescence detection

Nitrogen-containing functional groups can be used as a mediating factor for phosphorescence initiation in the probe. By removing nitrogen-containing functional groups, luminous transition metals and lanthanide complexes are released for HClO detection (Scheme 12).[109–113] Zhang *et al.* reported a transition metal complex phosphorescent probe Ru-Fc (49) for the detection of HClO *in vivo* with high sensitivity and selectivity.[109] In view of the classical photoinduced electron transfer inhibition luminescence principle, the metal-to-ligand charge transfer state of the [Ru(bpy)$_2$(COOH-bpy)]$^{2+}$ complex was re-established by HClO-promoted cleavage of the nitrogen-containing moiety, resulting in remarkable photoluminescence emission. Due to its lower cytotoxicity and distribution in the lysosome by intracellular endocytosis, this probe allowed one to monitor HClO in the lysosome of living cells and in liver injury of zebrafish using confocal microscopy and flow cytometry. By replacing Ru(ii) with Ir(iii), another phosphorescent probe Ir-Fc (50) was synthesized with the same HClO response group.[110] Notably, this probe enabled HClO to be imaged by single-photon, two-photon and lifetime mode in liver injury of mice and living cells.

Sun *et al.* synthesized a dinuclear Ru(ii) complex phosphorescent probe Ruazo (51) for HClO by combining the azo-*o*-amino moiety with the Ru(ii) complex.[111] A highly luminescent product was formed by the oxidation of azo-*o*-amino groups in the binuclear ruthenium(ii) complex. The synergetic effect of the dinuclear Ru(ii) complex could improve the sensitivity and selectivity for HClO. Thus, the probe imaged HClO inside living cells and mice. In addition, Chao *et al.* synthesized a series of Ir(iii) complex multicolor probes Ir1-Ir4 (52) by coupling the diaminomaleonitrile moiety with the bipyridine ligand in the Ir(iii) center for sensing HClO.[112] By the elimination of C=N isomerization, the probe could turn on phosphorescence emission from 534 nm to 598 nm. These multicolor emissions of these probes facilitated the visualization of HClO inside the mitochondria of living cells.

Scheme 12 Structures and mechanisms of nitrogen-containing functional group probes for HClO/ClO⁻. Reprinted with permission from ref. 109. Copyright 2015, Elsevier. Reprinted with permission from ref. 110. Copyright 2017, Elsevier. Reprinted with permission from ref. 111. Copyright 2016, Nature. Reprinted with permission from ref. 112. Copyright 2014, Royal Society of Chemistry. Reprinted with permission from ref. 113. Copyright 2015, Royal Society of Chemistry.

The C=N isomerization was also useful for the development of nanomaterial-based phosphorescent probes. For example, Huang et al. prepared a silica-based core-shell ratio phosphorescent nanoprobe SiO$_2$-1@mSiO$_2$-2.[113] This nanoprobe showed no-luminescence because the C=N isomerization of complex (53) resulted in non-radiative decay of the excited state. Once exposed to ClO$^-$, the luminescence of the nanoprobe varied dramatically from blue to red. Therefore, the intracellular detection of exogenous and endogenous ClO$^-$ was demonstrated via ratiometric imaging and photoluminescence lifetime imaging microscopy.
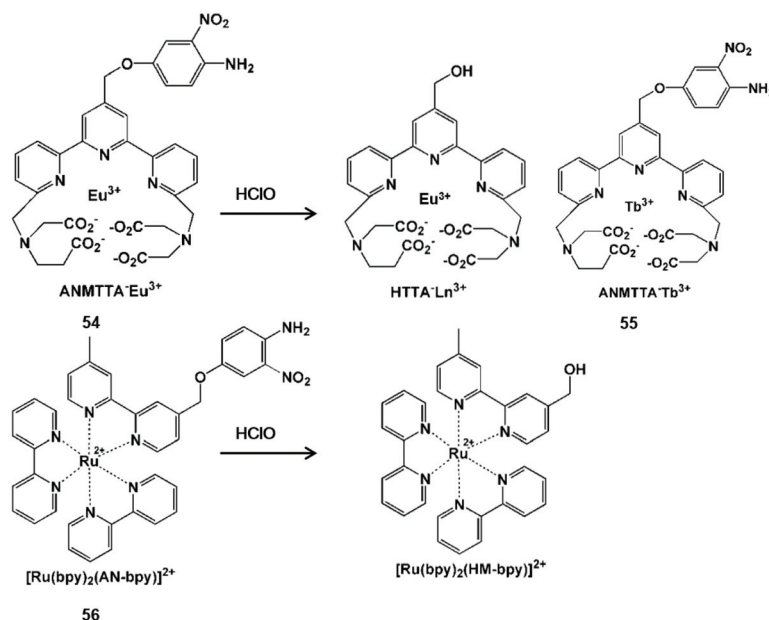
Oxygen-containing functional groups for HClO/ClO$^-$ phosphorescence detection

The oxidative cracking reaction of ether groups can enhance phosphorescence intensity or change the luminous wavelength of the probe (Scheme 13). In 2012, Yuan et al. synthesized a group of time-gated luminescent probes ANMTTA-Eu^{3+}, ANMTTA-Tb^{3+} and ANMTTA-Ln^{3+} for the specific detection of HClO.[114] In these probes, the photoinduced electron transfer process regulated the luminescence emission of the probe. The cleavage of the ether group can block the photoinduced electron transfer, resulting in the long-lived (millisecond) luminescence of the lanthanide HTTA-Eu^{3+}/Tb^{3+} complex. In comparison with ANMTTA-Tb^{3+} (55) probes, the ANMTTA-Eu^{3+} (54) probe exhibited excellent selectivity towards HClO, enabling it to be used for the detection of HClO secreted in live cells by time-gated luminescence imaging without background. Similarly, Yuan and his co-authors synthesized another probe [Ru(bpy)$_2$(AN-bpy)]$^{2+}$ (56) by introducing the same HClO recognition moiety for the real-time detection of HClO.[115] This probe showed fast response to HClO, leading to the 110-fold luminescence enhancement in the oxidation product of [Ru(bpy)$_2$(HM-bpy)]$^{2+}$. In addition to the imaging of the exogenous HClO in HeLa cells, the endogenous HClO generation at porcine neutrophils was also observed in microscopy images. The signal output of the single emission probe usually was interfered by analyte-independent factors. In order to break the limit, Yuan et al. further constructed a silica-based core-shell ratiometric time-gated luminescent nanoprobe RTLNP.[116] In this probe, the β-diketonate Eu^{3+} complex was coated on the surface of silica nanoparticles for specifically sensing HClO and the green emission of the Tb^{3+} complex acted as a reference signal (Fig. 6). Therefore, the ratio phosphorescence emission was exhibited by the oxidation of β-diketonate. This long-lived phosphorescent emission enabled the probe to accurately and sensitively detect HClO in living cells and animals via ratiometric time-gated luminescence imaging microscopy.

Unsaturated double bonds for HClO/ClO$^-$ phosphorescence detection

In general, unsaturated double bonds of the probe can be broken or form carboxylic acid upon action with HClO (Scheme 14).[117,118] Khatua et al. synthesized a bis-heteroleptic Ru(II) complex based phosphorescent probe Ru-1 with the 1,2,3-triazole ligand, which achieved the conversion from C=C bond to C–H hydroxylation to detect HClO.[117] C(sp^2)–H hydroxylation of this complex could inhibit the nonradiative decay of the excited state Ru-1 (57) and turn on the luminescence of Ru-1-OH/O$^-$. Due to the advantages of membrane penetrability and low cytotoxicity, this probe was used for HClO imaging in HEK293T cells. In addition, Yuan and his co-workers synthesized a functional lanthanide complex probe by

Scheme 13 Structures and mechanisms of oxygen-containing functional group probes for HClO/ClO$^-$. Reprinted with permission from ref. 114. Copyright 2012, American Chemical Society. Reprinted with permission from ref. 115. Copyright 2014, Royal Society of Chemistry.
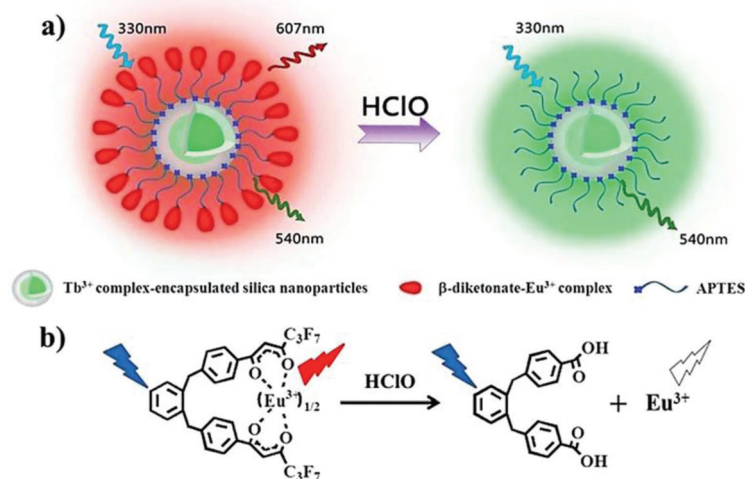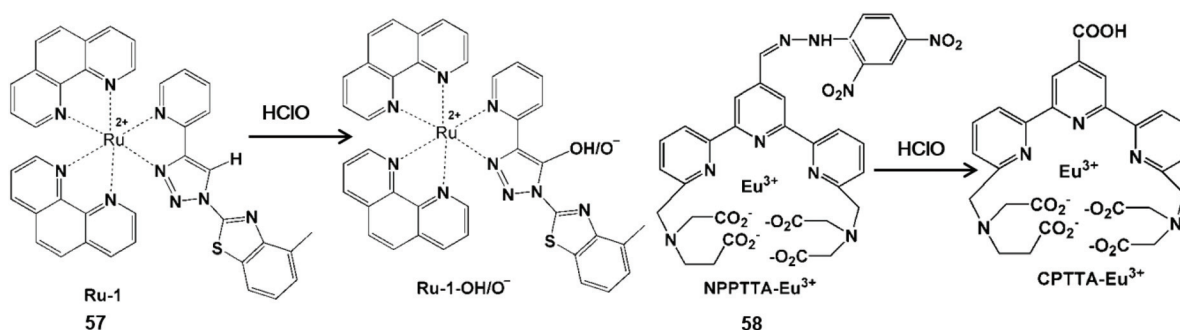
Fig. 6 Design concept of a ratiometric luminescent probe based on crow-like dual-emissive silica nanoparticles modified by Tb^{3+} and Eu^{3+} complexes (a), and the luminescence quenching mechanism of a β-diketonate-Eu^{3+} complex by HClO (b). Reprinted with permission from ref. 115. Copyright 2017, Royal Society of Chemistry.

Scheme 14 Structures and mechanisms of unsaturated double bond-containing functional group probes for $HClO/ClO^-$. Reprinted with permission from ref. 117. Copyright 2019, American Chemical Society. Reprinted with permission from ref. 118. Copyright 2017, Institute of Physics.

incorporating dinitrophenyl into a terpyridine polyacid (NPPTA)-Eu^{3+} complex (58) through a hydrazine linker for HClO.[118] Nitro groups were cracked by HClO to generate the strong luminescent Eu^{3+} complex, accompanied by a 900-fold luminescence enhancement with a long lifetime of 1.41 ms. Hence, the visualizations of HClO generated in RAW264.7 cells and Daphnia Magna were performed by time-gated luminescence imaging technology.

Chemiluminescent probes for HClO/ClO⁻ detection

Chemiluminescence is the process of converting chemical energy into luminescence.[119] Recently, probe-based chemiluminescence has been widely explored for determination systems due to merits such as no background signal, no photobleaching, simple equipment and fast signal response.[120–122] Moreover, chemiluminescence can accurately detect analytes

online and avoid the transformation of analytes in the subsequent reactions.[123] On account of the high signal-to-noise ratio, probe-based chemiluminescence imaging plays a very important role in the fields of immunology and cell biology.[124,125] Chemiluminescent probes for detecting HClO/ClO⁻ *in vivo* have been reported. In addition to direct luminescence, indirect luminescence including chemiluminescence resonance energy transfer can be used to enhance the luminescence intensity and improve the detection sensitivity for HClO/ClO⁻. Table 3 summarizes chemiluminescent probes for HClO/ClO⁻ by comparing their emission wavelengths, detection limits and imaging applications.

Conjugated polymers can be used as energy receptors in chemiluminescence resonance energy transfer to enhance chemiluminescence with their characteristics of optical signal amplification and light capture.[126,127] Therefore, Duan *et al.* designed a conjugated polymer-based chemiluminescence nanoprobe CPN-PFV-*co*-MEHPV (59) for imaging ClO⁻ *in vivo*.[128] The C=C bond of polyfluorene-vinylene (PFV) can

Table 3 Summary of different chemiluminescent probes for HClO/ClO⁻ detection

Probe	λ_{em} (nm)	Linear range (μM)	LOD (μM)	Imaging application	Ref.
CPN-PFV-*co*-MEHPV (59)	560	2–30	0.47	Mice	128
Benzoylhydrazine luciferin (60)	560	0–62.5	0.705	MDA-MB-231 cells, nude mice	130
D-Luciferin cage (61)	560	1–200	0.033	ES-2-Fluc cells and mice	131

Scheme 15 Structures and mechanism of chemiluminescent probes for HClO/ClO⁻. Reprinted with permission from ref. 128. Copyright 2018, American Chemical Society. Reprinted with permission from ref. 130. Copyright 2017, American Chemical Society. Reprinted with permission from ref. 131. Copyright 2018, Royal Society of Chemistry.

form high energy intermediates through ClO⁻-mediated π^2–π^2 cycloaddition. Because of the instability of the intermediate, it can transfer energy to the conjugated polymer receptor, along with long-lived chemiluminescence (half-life 3.0 min). Using this chemiluminescent probe, endogenous ClO⁻ generation in a mouse model of peritonitis inflammation was imaged.

Bioluminescence is a special type of chemiluminescence in biological systems.[129] Liang *et al.* developed a benzoylhydrazine luciferin bioluminescent probe (60) for the highly selective detection of ClO⁻ *in vivo*.[130] In this report, the carboxyl group of this probe was oxidized by ClO⁻ and hydrolyzed to release D-luciferin, which was used for luciferase to generate light signals. This bioluminescent probe has been utilized for bioimaging of ClO⁻ in live cells and tumors. Similarly, Li *et al.* designed two kinds of turn-on bioluminescent probes (61) for the selective detection of ClO⁻ by using a versatile and well-

implemented caging D-luciferin strategy.[131] By the interaction with ClO⁻, sulfide and the tetraminophenol moiety masking groups were cleaved to yield D-luciferin for luciferase to generate a light readout. Therefore, this probe was applied for the highly selective detection of ClO⁻ *in vitro* and imaging endogenous ClO⁻ in a mouse inflammation model. The HClO/ClO⁻ detection mechanisms of the above chemiluminescent probes are shown in Scheme 15.

Conclusion and prospective

The detection of HClO/ClO⁻ *in vitro* and *in vivo* is essential for biological applications, especially in biomedicine. The development of luminescent probes is conductive for people to intuitively locate the lesions caused by HClO/ClO⁻, and further

to explore the effects of HClO/ClO⁻ on physiological functions of living organisms. In this review, we discussed the detection mechanisms of luminescent probes for HClO/ClO⁻ with different recognition groups. Among them, fluorescent and phosphorescent probes have been widely used for the localization and detection of HClO/ClO⁻ *in vitro* and *in vivo*. In order to make up for the oneness and deficiency of the above probes, other probes for HClO/ClO⁻ have also been developed. Two-photon/near-infrared fluorescent probes have a strong ability to penetrate biological tissues and avoid damage to biological samples, but still cannot completely avoid the detriment of incident light. Chemiluminescent probes can be activated to allow the real-time monitoring of HClO/ClO⁻ *in vitro* and *in vivo* without external light. However, the luminescence intensity and lifetime of chemiluminescent probes limit their further applications.

Nowadays, great progress has been made in the research of luminescent probes in HClO/ClO⁻. However, there are still some challenges in clinical applications. Furthermore, most of the luminescent probes described in this review are irreversible. Therefore, it is a critical criterion to further explore the comprehensiveness of the detection performance of the luminescent probes. In view of the superior contribution to biological detection, we believe that luminescent probes will continue to make new progress in the field of biological analysis.

Conflicts of interest

There are no conflicts to declare.

Acknowledgements

Notes and references

1 J. Zielonka, J. Joseph, A. Sikora, M. Hardy, O. Ouari, J. Vasquez-Vivar, G. Cheng, M. Lopez and B. Kalyanaraman, *Chem. Rev.*, 2017, **117**, 10043–10120.
2 Y. He, Y. Xu, Y. Shang, S. Zheng, W. Chen and Y. Pang, *Anal. Bioanal. Chem.*, 2018, **410**, 7007–7017.
3 M. Ren, K. Zhou, L. He and W. Lin, *J. Mater. Chem. B*, 2018, **6**, 1716–1733.
4 E. Hidalgo, R. Bartolome and C. Dominguez, *Chem.-Biol. Interact.*, 2002, **139**, 265–282.
5 C. Jiao, Y. Liu, J. Pang, W. Lu, P. Zhang and Y. Wang, *J. Photochem. Photobiol., A*, 2020, **392**, 112399.
6 Y.-X. Liao, M.-D. Wang, K. Li, Z.-X. Yang, J.-T. Hou, M.-Y. Wu, Y.-H. Liu and X.-Q. Yu, *RSC Adv.*, 2015, **5**, 18275–18278.
7 L. Gebicka and E. Banasiak, *Toxicol. in Vitro*, 2012, **26**, 924–929.
8 S. Baldus, C. Heeschen, T. Meinertz, A. M. Zeiher, J. P. Eiserich, T. Münzel, M. L. Simoons and C. W. Hamm, *Circulation*, 2003, **108**, 1440–1445.
9 J. Perez-Vilar and R. C. Boucher, *Free Radicals Biol. Med.*, 2004, **37**, 1564–1577.
10 J. K. Andersen, *Nat. Med.*, 2004, **10**, S18–S25.
11 S. Parvez, M. J. C. Long, J. R. Poganik and Y. Aye, *Chem. Rev.*, 2018, **118**, 8798–8888.
12 L. Wu, A. C. Sedgwick, X. Sun, S. D. Bull, X.-P. He and T. D. James, *Acc. Chem. Res.*, 2019, **52**, 2582–2597.
13 P. S. Francis, N. W. Barnett, S. W. Lewis and K. F. Lim, *Luminescence*, 2004, **19**, 94–115.
14 X. Wang, H. Chang, J. Xie, B. Zhao, B. Liu, S. Xu, W. Pei, N. Ren, L. Huang and W. Huang, *Coord. Chem. Rev.*, 2014, **273**, 201–212.
15 S. Samanta, S. Goswami, Md. N. Hoque, A. Ramesh and G. Das, *Chem. Commun.*, 2014, **50**, 11833–11836.
16 S. Singha, Y. W. Jun, S. Sarkar and K. H. Ahn, *Acc. Chem. Res.*, 2019, **52**, 2571–2581.
17 X. Wu, Z. Li, L. Yang, J. Han and S. Han, *Chem. Sci.*, 2013, **4**, 460–467.
18 H. Xiao, J. Li, J. Zhao, G. Yin, Y. Quan, J. Wang and R. Wang, *J. Mater. Chem. B*, 2015, **3**, 1633–1638.
19 X. Cheng, H. Jia, T. Long, J. Feng, J. Qin and Z. Li, *Chem. Commun.*, 2011, **47**, 11978–11980.
20 Y. He, C. Fan and S.-T. Lee, *Nano Today*, 2010, **5**, 282–295.
21 Q. Mei, W. Deng, W. Yisibashaer, H. Jing, G. Du, M. Wu, B. N. Li and Y. Zhang, *Small*, 2015, **11**, 4568–4575.
22 J. J. Hu, S. Ye and D. Yang, *Isr. J. Chem.*, 2017, **57**, 251–258.
23 H. Kobayashi, M. Ogawa, R. Alford, P. L. Choyke and Y. Urano, *Chem. Rev.*, 2010, **110**, 2620–2640.
24 M. Yu, F. Li, Z. Chen, H. Hu, C. Zhan, H. Yang and C. Huang, *Anal. Chem.*, 2009, **81**, 930–935.
25 X. Chen, X. Tian, I. Shin and J. Yoon, *Chem. Soc. Rev.*, 2011, **40**, 4783–4804.
26 X. Xu, P. E. Saw, W. Tao, Y. Li, X. Ji, S. Bhasin, Y. Liu, D. Ayyash, J. Rasmussen, M. Huo, J. Shi and O. C. Farokhzad, *Adv. Mater.*, 2017, **29**, 1700141.
27 D. Liu, M. Zhang, W. Du, L. Hu, F. Li, X. Tian, A. Wang, Q. Zhang, Z. Zhang, J. Wu and Y. Tian, *Inorg. Chem.*, 2018, **57**, 7676–7683.
28 J. Chen, X. Jiang, C. Zhang, K. R. MacKenzie, F. Stossi, T. Palzkill, M. C. Wang and J. Wang, *ACS Sens.*, 2017, **2**, 1257–1261.
29 Q. Meng, H. Jia, P. Succar, L. Zhao, R. Zhang, C. Duan and Z. Zhang, *Biosens. Bioelectron.*, 2015, **74**, 461–468.
30 R. Zhang, B. Song and J. Yuan, *Trends Anal. Chem.*, 2018, **99**, 1–33.
31 D. Wu, L. Chen, Q. Xu, X. Chen and J. Yoon, *Acc. Chem. Res.*, 2019, **52**, 2158–2168.
32 S. Kenmoku, Y. Urano, H. Kojima and T. Nagano, *J. Am. Chem. Soc.*, 2007, **129**, 7313–7318.
33 Y. Koide, Y. Urano, K. Hanaoka, T. Terai and T. Nagano, *J. Am. Chem. Soc.*, 2011, **133**, 5680–5682.

34 X. Chen, K.-A. Lee, E.-M. Ha, K. M. Lee, Y. Y. Seo, H. K. Choi, H. N. Kim, M. J. Kim, C.-S. Cho, S. Y. Lee, W.-J. Lee and J. Yoon, *Chem. Commun.*, 2011, **47**, 4373–4375.

35 J. Zhou, L. Li, W. Shi, X. Gao, X. Li and H. Ma, *Chem. Sci.*, 2015, **6**, 4884–4888.

36 A. Manna, D. Sarkar, S. Goswami, C. K. Quah and H.-K. Fun, *RSC Adv.*, 2016, **6**, 57417–57423.

37 T. C. Stadtman, *Annu. Rev. Biochem.*, 1980, **49**, 93–110.

38 R. F. Burk, *Nutr. Clin. Care*, 2002, **5**, 75–79.

39 B. Wang, P. Li, F. Yu, P. Song, X. Sun, S. Yang, Z. Lou and K. Han, *Chem. Commun.*, 2013, **49**, 1014–1016.

40 S.-R. Liu and S.-P. Wu, *Org. Lett.*, 2013, **15**, 878–881.

41 G. Cheng, J. Fan, W. Sun, J. Cao, C. Hu and X. Peng, *Chem. Commun.*, 2014, **50**, 1018–1020.

42 Y. L. Pak, S. J. Park, Q. Xu, H. M. Kim and J. Yoon, *Anal. Chem.*, 2018, **90**, 9510–9514.

43 Q. Xu, C. H. Heo, G. Kim, H. W. Lee, H. M. Kim and Y. Yoon, *Angew. Chem., Int. Ed.*, 2015, **54**, 4890–4894.

44 Q. Xu, C. H. Heo, J. A. Kim, H. S. Lee, Y. Hu, D. Kim, K. M. K. Swamy, G. Kim, S.-J. Nam, H. M. Kim and J. Yoon, *Anal. Chem.*, 2016, **88**, 6615–6620.

45 L. Yuan, L. Wang, B. K. Agrawalla, S. J. Park, H. Zhu, B. Sivaraman, J. Peng, Q.-H. Xu and Y.-T. Chang, *J. Am. Chem. Soc.*, 2015, **137**, 5930–5938.

46 G. Li, D. Zhu, Q. Liu, L. Xue and H. Jiang, *Org. Lett.*, 2013, **15**, 2002–2005.

47 P. Zhang, H. Wang, D. Zhang, X. Zeng, R. Zeng, L. Xiao, H. Tao, Y. Long, P. Yi and J. Chen, *Sens. Actuators, B*, 2018, **255**, 2223–2231.

48 P. Zhang, H. Wang, Y. Hong, M. Yu, R. Zeng, Y. Long and J. Chen, *Biosens. Bioelectron.*, 2018, **99**, 318–324.

49 Y. Zhou, W. Pei, C. Wang, J. Zhu, J. Wu, Q. Yuan, L. Wang, W. Huang, C. Yao, J. S. C. Loo and Q. Zhang, *Small*, 2014, **10**, 3560–3567.

50 G. Wu, F. Zeng and S. Wu, *Anal. Methods*, 2013, **5**, 5589–5596.

51 Y. Ding, C. Xu, Z. Li, W. Qin, X. Han, X. Han, C. Zhang, C. Yu, X. Wang, L. Li and W. Huang, *ChemBioChem*, 2019, **20**, 831–837.

52 G. Cheng, J. Fan, W. Sun, K. Sui, X. Jin, J. Wang and X. Peng, *Analyst*, 2013, **138**, 6091–6096.

53 S. I. Reja, V. Bhalla, A. Sharma, G. Kaur and M. Kumar, *Chem. Commun.*, 2014, **50**, 11911–11914.

54 M. Ren, B. Deng, K. Zhou, X. Kong, J.-Y. Wang, G. Xu and W. Lin, *J. Mater. Chem. B*, 2016, **4**, 4739–4745.

55 L. Yuan, W. Lin, Y. Xie, B. Chen and J. Song, *Chem. – Eur. J.*, 2012, **18**, 2700–2706.

56 H. Li, X. Li, X. Wu, W. Shi and H. Ma, *Anal. Chem.*, 2017, **89**, 5519–5525.

57 B. Zhu, M. Zhang, L. Wu, Z. Zhao, C. Liu, Z. Wang, Q. Duan, Y. Wang and P. Jia, *Sens. Actuators, B*, 2018, **257**, 436–441.

58 D. Liu, S. Feng and G. Feng, *Sens. Actuators, B*, 2018, **269**, 15–21.

59 C. Liu, Z. Li, C. Yu, Y. Chen, D. Liu, Z. Zhuang, P. Jia, H. Zhu, X. Zhang, Y. Yu, B. Zhu and W. Sheng, *ACS Sens.*, 2019, **4**, 2156–2163.

60 Y. Xia, X. Liu, D. Wang, Z. Wang, Q. Liu, H. Yu, M. Zhang and Y. Song, *Chin. Chem. Lett.*, 2018, **29**, 1517–1520.

61 Z. Zhan, R. Liu, L. Chai, Q. Li, K. Zhang and Y. Lv, *Anal. Chem.*, 2017, **89**, 9544–9551.

62 Y. Koide, Y. Urano, S. Kenmoku, H. Kojima and T. Nagano, *J. Am. Chem. Soc.*, 2007, **129**, 10324–10325.

63 J. Shepherd, S. A. Hilderbrand, P. Waterman, J. W. Heinecke, R. Weissleder and P. Libby, *Chem. Biol.*, 2007, **14**, 1221–1231.

64 T. Guo, L. Cui, J. Shen, R. Wang, W. Zhu, Y. Xu and X. Qian, *Chem. Commun.*, 2013, **49**, 1862–1864.

65 A. N. Chermahini, B. Hosseinzadeh, A. S. Beni and A. Teimouri, *Comput. Theor. Chem.*, 2012, **994**, 97–104.

66 X.-F. Zhang and N. Feng, *Spectrochim. Acta, Part A*, 2018, **189**, 13–21.

67 J. F. Callan, A. P. de Silva and D. C. Magri, *Tetrahedron*, 2005, **61**, 8551–8588.

68 H. Zhu, J. Fan, J. Wang, H. Mu and X. Peng, *J. Am. Chem. Soc.*, 2014, **136**, 12820–12823.

69 J. Fan, H. Mu, H. Zhu, J. Du, N. Jiang, J. Wang and X. Peng, *Ind. Eng. Chem. Res.*, 2015, **54**, 8842–8846.

70 J. Zhou, Z. Cao, N. Panwar, R. Hu, X. Wang, J. Qu, S. C. Tjin, G. Xu and K.-T. Yong, *Coord. Chem. Rev.*, 2017, **352**, 15–66.

71 K. Sun, X. Li, X. Yu, L. Liu, Q. Meng, F. Wang and R. Zhang, *J. Colloid Interface Sci.*, 2017, **486**, 128–135.

72 L. Liang, A. Care, R. Zhang, Y. Lu, N. H. Packer, A. Sunna, Y. Qian and A. V. Zvyagin, *ACS Appl. Mater. Interfaces*, 2016, **8**, 11945–11953.

73 H. Zhu, H. Xu, Y. Yan, K. Zhang, T. Yu, H. Jiang and S. Wang, *Sens. Actuators, B*, 2014, **202**, 667–673.

74 D. E. Sosnovik, M. Nahrendorf, N. Deliolanis, M. Novikov, E. Aikawa, L. Josephson, A. Rosenzweig, R. Weissleder and V. Ntziachristos, *Circulation*, 2007, **115**, 1384–1391.

75 M. Harisinghani, R. W. Ross, A. R. Guimaraes and R. Weissleder, *Neoplasia*, 2007, **9**, 1160–1165.

76 P. Panizzi, M. Nahrendorf, M. Wildgruber, P. Waterman, J.-L. Figueiredo, E. Aikawa, J. M. Carthy, R. Weissleder and S. A. Hilderbrand, *J. Am. Chem. Soc.*, 2009, **131**, 15739–15744.

77 T.-H. Wu, C.-P. Liu, C.-T. Chien and S.-Y. Lin, *Chem. – Eur. J.*, 2013, **19**, 11672–11675.

78 H. Wang, Y. Li, Y. Chen, L. Li, T. Fang and Z. Tang, *J. Mater. Chem. C*, 2015, **3**, 5136–5140.

79 P. Zhang, J. Li, B. Li, J. Xu, F. Zeng, J. Lv and S. Wu, *Chem. Commun.*, 2015, **51**, 4414–4416.

80 Y. Huang, P. Zhang, M. Gao, F. Zeng, A. Qin, S. Wu and B. Z. Tang, *Chem. Commun.*, 2016, **52**, 7288–7291.

81 X. Li, J. Gu, Z. Zhou, W. Liu, J. Gao and Q. Wang, *Dyes Pigm.*, 2020, **172**, 107844.

82 C. Cao, X. Zhou, M. Xue, C. Han, W. Feng and F. Li, *ACS Appl. Mater. Interfaces*, 2019, **11**, 15298–15305.

83 G. Chen, F. Song, J. Wang, Z. Yang, S. Sun, J. Fan, X. Qiang, X. Wang, B. Dou and X. Peng, *Chem. Commun.*, 2012, **48**, 2949–2951.

84 G. Hong, S. Diao, A. L. Antaris and H. Dai, *Chem. Rev.*, 2015, **115**, 10816–10906.

85 Y. Zhan, F. Luo, L. Guo, B. Qiu, Y. Lin, J. Li, G. Chen and Z. Lin, *ACS Sens.*, 2017, **2**, 1684–1691.

86 V. Biju, T. Itoh and M. Ishikawa, *Chem. Soc. Rev.*, 2010, **39**, 3031–3056.

87 Y.-C. Yang, H.-H. Lu, W.-T. Wang and I. Liau, *Anal. Chem.*, 2011, **83**, 8267–8272.

88 Z.-N. Sun, F.-Q. Liu, Y. Chen, P. K. H. Tam and D. Yang, *Org. Lett.*, 2008, **10**, 2171–2174.

89 J. J. Hu, N.-K. Wong, Q. Gu, X. Bai, S. Ye and D. Yang, *Org. Lett.*, 2014, **16**, 3544–3547.

90 Z. Zhou, J. Gu, X. Qiao, H. Wu, H. Fu, L. Wang, H. Li and L. Ma, *Sens. Actuators, B*, 2019, **282**, 437–442.

91 Z. Zhou, H. Wu, F. Li, L. Ma and X. Qiao, *Dyes Pigm.*, 2020, **174**, 108033.

92 M. Sun, H. Yu, H. Zhu, F. Ma, S. Zhang, D. Huang and S. Wang, *Anal. Chem.*, 2014, **86**, 671–677.

93 L. Yuan, W. Lin, J. Song and Y. Yang, *Chem. Commun.*, 2011, **47**, 12691–12693.

94 L.-L. Xi, X.-F. Guo, C.-L. Wang, W.-L. Wu, M.-F. Huang, J.-Y. Miao and B.-X. Zhao, *Sens. Actuators, B*, 2018, **255**, 666–671.

95 D.-P. Li, Z.-Y. Wang, X.-J. Cao, J. Cui, X. Wang, H.-Z. Cui, J.-Y. Miao and B.-X. Zhao, *Chem. Commun.*, 2016, **52**, 2760–2763.

96 Z. Gao, X. Zhang, M. Zheng and Y. Chen, *Dyes Pigm.*, 2015, **120**, 37–43.

97 C. Xu and Y. Qian, *Dyes Pigm.*, 2019, **161**, 303–312.

98 H. Xiong, L. He, Y. Zhang, J. Wang, X. Song and Z. Yang, *Chin. Chem. Lett.*, 2019, **30**, 1075–1077.

99 Y. Wu, J. Wang, F. Zeng, S. Huang, J. Huang, H. Xie, C. Yu and S. Wu, *ACS Appl. Mater. Interfaces*, 2016, **8**, 1511–1519.

100 J. Zha, B. Fu, C. Qin, L. Zeng and X. Hu, *RSC Adv.*, 2014, **4**, 43110–43113.

101 J. Rena, P. Zhanga, H. Liu, C. Zhang, Y. Gao, J. Cui and J. Chen, *Sens. Actuators, B*, 2020, **304**, 127299.

102 Q. Gao, W. Zhang, B. Song, R. Zhang, W. Gou and J. Yuan, *Anal. Chem.*, 2017, **89**, 4517–4524.

103 M. L. Aulsebrook, B. Graham, M. R. Grace and K. L. Tuck, *Coord. Chem. Rev.*, 2018, **375**, 191–220.

104 K. K.-W. Lo, A. W.-T. Choi and S. P.-Y. Li, *Dalton Trans.*, 2012, **41**, 6021–6047.

105 K. Y. Zhang, Q. Yu, H. Wei, S. Liu, Q. Zhao and W. Huang, *Chem. Rev.*, 2018, **118**, 1770–1839.

106 R. Zhang, Z. Ye, B. Song, Z. Dai, X. An and J. Yuan, *Inorg. Chem.*, 2013, **52**, 10325–10331.

107 X. Liu, Z. Tang, B. Song, H. Ma and J. Yuan, *J. Mater. Chem. B*, 2017, **5**, 2849–2855.

108 F. Liu, Y. Gao, J. Wang and S. Sun, *Analyst*, 2014, **139**, 3324–3329.

109 L. Cao, R. Zhang, W. Zhang, Z. Du, C. Liu, Z. Ye, Bo Song and J. Yuan, *Biomaterials*, 2015, **68**, 21–31.

110 F. Zhang, X. Liang, W. Zhang, Y.-L. Wang, H. Wang, Y. H. Mohammed, B. Song, R. Zhang and J. Yuan, *Biosens. Bioelectron.*, 2017, **87**, 1005–1011.

111 Z. Liu, K. Gao, B. Wang, H. Yan, P. Xing, C. Zhong, Y. Xu, H. Li, J. Chen, W. Wang and S. Sun, *Sci. Rep.*, 2016, **6**, 29065.

112 G. Li, Q. Lin, L. Ji and H. Chao, *J. Mater. Chem. B*, 2014, **2**, 7918–7926.

113 K. Y. Zhang, J. Zhang, Y. Liu, S. Liu, P. Zhang, Q. Zhao, Y. Tang and W. Huang, *Chem. Sci.*, 2015, **6**, 301–307.

114 Y. Xiao, R. Zhang, Z. Ye, Z. Dai, H. An and J. Yuan, *Anal. Chem.*, 2012, **84**, 10785–10792.

115 Z. Ye, R. Zhang, B. Song, Z. Dai, D. Jin, E. M. Goldys and J. Yuan, *Dalton Trans.*, 2014, **43**, 8414–8420.

116 H. Ma, B. Song, Y. Wang, D. Cong, Y. Jiang and J. Yuan, *Chem. Sci.*, 2017, **8**, 150–159.

117 B. Sen, S. K. Sheet, S. K. Patra, D. Koner, N. Saha and S. Khatua, *Inorg. Chem.*, 2019, **58**, 9982–9991.

118 X. Liu, L. Guo, B. Song, Z. Tang and J. Yuan, *Methods Appl. Fluoresc.*, 2017, **5**, 014009.

119 W. Adam, D. V. Kazakov and V. P. Kazakov, *Chem. Rev.*, 2005, **105**, 3371–3387.

120 X. Liu, R. Freeman, E. Golub and I. Willner, *ACS Nano*, 2011, **5**, 7648–7655.

121 H. Zhang, X. Zhang and S. Dong, *Anal. Chem.*, 2015, **87**, 11167–11170.

122 N. Siraj, B. El-Zahab, S. Hamdan, T. E. Karam, L. H. Haber, M. Li, S. O. Fakayode, S. Das, B. Valle, R. M. Strongin, G. Patonay, H. O. Sintim, G. A. Baker, A. Powe, M. Lowry, J. O. Karolin, C. D. Geddes and I. M. Warner, *Anal. Chem.*, 2016, **88**, 170–202.

123 A. S. Calbry-Muzyka, J. Indlekofer, J. Schneebeli and S. M. A. Biollaz, *Energy Fuels*, 2019, **33**, 9859–9869.

124 J. Li, J. Rao and K. Pu, *Biomaterials*, 2018, **155**, 217–235.

125 Y. Xia, R. Zhang, Z. Wang, J. Tian and X. Chen, *Chem. Soc. Rev.*, 2017, **46**, 2824–2843.

126 X. Duan, L. Liu, F. Feng and S. Wang, *Acc. Chem. Res.*, 2010, **43**, 260–270.

127 J. Wang, F. Lv, L. Liu, Y. Ma and S. Wang, *Coord. Chem. Rev.*, 2018, **354**, 135–154.

128 B. Zhu, W. Tang, Y. Ren and X. Duan, *Anal. Chem.*, 2018, **90**, 13714–13722.

129 L. J. Kricka and G. H. G. Thorpe, *Analyst*, 1983, **108**, 1274–1296.

130 P. Chen, Z. Zheng, Y. Zhu, Y. Dong, F. Wang and G. Liang, *Anal. Chem.*, 2017, **89**, 5693–5696.

131 C. Tang, Y. Gao, T. Liu, Y. Lin, X. Zhang, C. Zhang, X. Li, T. Zhang, L. Du and M. Li, *Org. Biomol. Chem.*, 2018, **16**, 645–651.